SHIELDING EFFECTIVENESS OF PLASTIC MATERIALS FOR 5G APPLICATIONS

Andrea Amaro Pérez
Adrián Suárez Zapata
Pedro A. Martínez Delgado
Abraham Menéndez Márquez
Jorge Victoria Ahuir
José Torres País

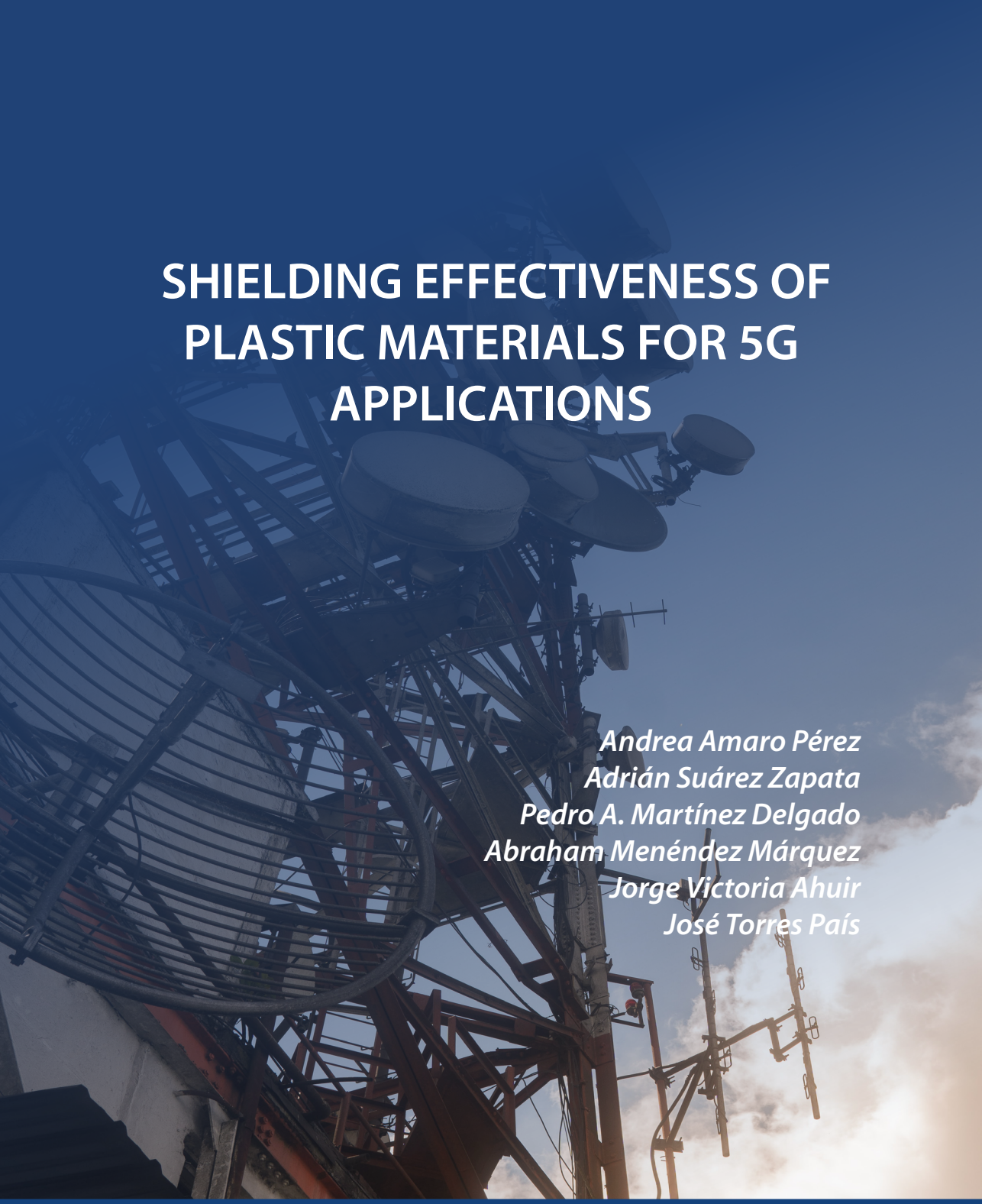

Ingeniería y Tecnología

3ciencias

SHIELDING EFFECTIVENESS OF PLASTIC MATERIALS FOR 5G APPLICATIONS

Andrea Amaro Pérez
Adrián Suárez Zapata
Pedro A. Martínez Delgado
Abraham Menéndez Márquez
Jorge Victoria Ahuir
José Torres País

Editorial Área de Innovación y Desarrollo,S.L.

ÁREA DE INNOVACIÓN Y DESARROLLO, S.L.

Avda. Juan Gil Albert, 1 - 03802 - ALCOY (ALICANTE) info@3ciencias.com

Primera edición: **febrero 2022**

ISBN: **978-84-123872-5-4**

DOI: https://doi.org/10.17993/IngyTec.2022.79

ABSTRACT

The study and modelling of EMC are becoming more critical than ever due to the ubiquitous presence of electronic circuits in all aspects of our lives. Specifically, it is crucial to extend these studies to the new frequencies that, in a few years, will be a reality in modern telecommunications systems, such as 5G and its derived technologies. A specific critical field where the proper EMI shielding has been ensured to avoid EMC problems is the electric autonomous vehicles (EAVs). The huge number of electronics systems in new vehicles will dramatically extend the demands on the EMI shielding solutions used to attenuate the radiated emissions that could affect circuits in the vehicle. Metals or metal alloys are the most common EMI shielding materials since they demonstrate adequate shielding capacity against EMI. However, polymers have become up-and-coming materials for EMI shielding with the characteristics of lightweight, flexibility, cost-effective, easy processing, and resistance to corrosion.

Consequently, it is necessary to develop EMI shielding materials based on polymers, plastic materials, and fiber composites that ensure compliance with the different standards that regulate 5G and the proper operation of possible systems susceptible to the intentional and unintended signals generated by this new technology. This contribution focuses on characterizing different composite structures performance based on fibers combined with conductive materials in terms of shielding effectiveness, covering the 5G sub-6 GHz frequency range.

INDEX OF CONTENTS

CHAPTER I: INTRODUCTION

1.1. Project outline

This contribution is based on the study, measurement, and interpretation of shielding effectiveness results of polymer composites with characteristics proper to metallic materials. These materials are intended to replace conventional metallic materials in the field of EMC and EMI, especially in the 5G sub 6 GHz frequency range.

1.2. Objectives

The general objectives of this contribution are the design, manufacture, and characterization of materials for electromagnetic (EM) shielding in the 5G frequency range, such as in automotive industry applications. This general objective will be implemented through the following specific objectives:

- Study and characterization of the EM shielding properties of metallic and plastic materials in the 5G frequency range.
- Adaptation of the software for analyzing the EM properties of materials in the 5G frequency range.
- Study, design, and manufacture new plastic materials with EM shielding properties in the 5G frequency range.
- Study and characterize the shielding properties of the plastic materials developed in the 5G frequency range.
- Testing the properties of these new materials on components, systems, and equipment in the automotive sector.

1.3. Methodology

The first chapter aims to present the research project and its objectives. On the other hand, the context that frames the project will be set out to give rise to the following chapter.

Chapter two includes the theoretical aspects that the project is based on, starting with electromagnetic compatibility and ending with EMI Shielding.

Chapter three then describes the selection of materials measured in the project and gives a brief explanation of the manufacturing process, the structure, and the

modeling of the materials to understand the behavior of the materials.

Chapter four is dedicated to the measurement principle and the followed method to carry out all the measurements, as well as the measurement setup. In this chapter, the specific models of the equipment will be specified and the characteristics that make them suitable for this type of measurement will be discussed.

On the other hand, chapter five is dedicated to the LabVIEW software, presenting the software and the redesign of the specific driver for control and data acquisition with one of the devices used to carry out the preliminary measurements of the project. It also sets out the specifications that the driver must meet.

The sixth chapter contains the graphs and results of all the measurements carried out, as well as their interpretation. This chapter is divided according to the materials measured.

Finally, chapter seven contains the conclusions obtained from the project and the measurements, as well as briefly outlining the future lines of development that can be carried out along the lines of the project.

CHAPTER II: ANTECEDENTS AND STATE OF ART

2.1. Electromagnetic compatibility

Electromagnetic compatibility (EMC) is a discipline that ensures that electronic devices work properly in a given environment and proximity of other devices.

Before the mass distribution of electronic equipment, the receivers and radio transmitters were to operate in environments where the potential for interference came only from natural sources such as lightning, and almost nothing was done to minimize their susceptibility to external disturbances or to limit emissions. However, when they began to appear more and more artificial interference sources, it was necessary to further investigate and study the equipment malfunctions caused by these electromagnetic interferences.

This discipline acquired particular importance during the Second World War, when the military ships were equipped with complex electronic equipment and powerful, such as communication systems, radar and missiles, placed close to each other. It was also critical to understand the effects of the electromagnetic fields trigged by nuclear explosions on electronic devices.

Apart from its military applications, it soon became apparent that all electronics circuits have the possibility of radiating or picking up unwanted electrical interference which can compromise the operation of one or other of the circuits. Because of this, as early as in 1959 a Technical Committee of IEC (International Electrotechnical Commission) was proposed to cope with the needs of industry in semiconductor devices (IEC TC 47), including aspects of electromagnetic compatibility [1].

Electronic devices continually integrate more complex and more advanced functionalities. This involves the use of increasing operating frequencies, the miniaturization of the electronic design and high component integration, printed circuit board (PCB) size and thickness reduction, and using signals of very low voltage amplitude [2]. These design principles are often used to achieve a device with better performance and features; however, they increase the likelihood of generating complex electromagnetic interference (EMI) problems. The electronics can be sensitive to the surrounding electromagnetic environment, and it can also act as noise source, thus, it is very important to manage electromagnetic noise for avoiding unwanted electromagnetic interactions with nearby systems.

This problem is even more significant at gigahertz (GHz) frequency region since semiconductor elements and PCB tracks radiate electromagnetic interferences [3] [4][5]. Electromagnetic interference (EMI) has become a major problem for circuit designers, and it is likely to become even more severe in the future.

As a result of this growing realization, many nations became aware of EMC as a growing problem. Some started to issue directives to the manufacturers of electronic equipment, defining standards that the equipment should meet before equipment could be sold. The European Community was one for the first areas where EMC requirements were enforced. While many were skeptical at first, the introduction of EMC standards has raised standards and enabled most types of equipment to operate alongside each other without interference. This has been particularly important with the rapid growth in the use of mobile phones.

Noise interference occurs when three factors exist as indicated by the principal diagram in Fig. 1. First, there must be a noise source. Second, there must be a receptor circuit that is susceptible to the noise. Third, there must be a coupling channel to transmit the noise from the source to the receptor. In addition, the characteristics of the noise must be such that it is emitted at a frequency that the receptor is susceptible, an amplitude sufficient to affect the receptor, and a time the receptor is susceptible to the noise.

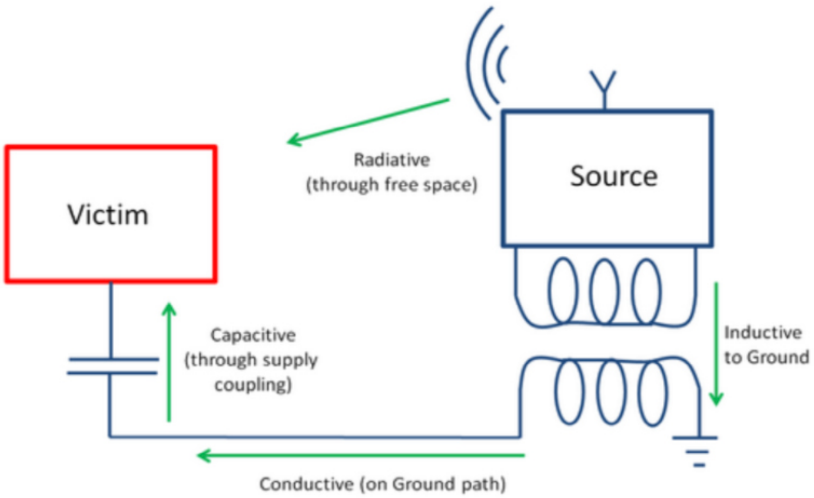

Figure 1. Representation of different types of EM interference.

Source: emisindia.com.

The different types of EM interference are described below:

- Radiated: This type of EMI coupling is the most common. It is the type of EMI that is normally experienced when the source and victim are separated by a large distance (typically more than a wavelength). The source radiates a signal which may be wanted or unwanted, and the victim receives it, which results in its improper performance.
- Conducted: Conducted emissions occur when there is a conduction route along which the signals can travel. This may be along power cables or other interconnection cabling. The conduction may be in one of two modes:
    - Common mode: This type of EMI coupling occurs when the noise appears in the same phase on the two conductors. A radiated field can couple to the system and induce any differential interference between the two wires of the cable. In the same way, the differential current will induce a radiated field of its own. The ground plane plays no role in this coupling.
    - Differential mode: This occurs when the noise is out of phase on the two conductors.
- Coupled: What is normally termed coupled EMI can be one of two forms, namely capacitive coupling and magnetic induction.
    - Capacitive coupling: This occurs when a changing voltage from the source capacitively transfers a charge to the victim circuitry.
    - Magnetic induction: This type of EMI coupling exists when a varying magnetic field exists between the source and victim. This induces a current in the victim circuitry, thereby transferring the signal from source to victim.

By determining the form of coupling that exists and the way in which it is reaching the victim, it may prove to be that the most effective method of reducing the EMI is by putting measures in place to reduce the coupling and reduce the level of interference to an acceptable level.

2.2. Electromagnetic noise

Electromagnetic noises can be classified into natural and artificial noises based on the source origin of electromagnetic noise as shown in the Fig. 2.

Natural noises are those that existed before the existence of electronic devices, for example, lightning and static electricity and, on the other hand, artificial noises are those resulting from the use of electronic devices. As electronic devices have become more and more commonly used, the interference caused by artificial noise has increased considerably in recent years.

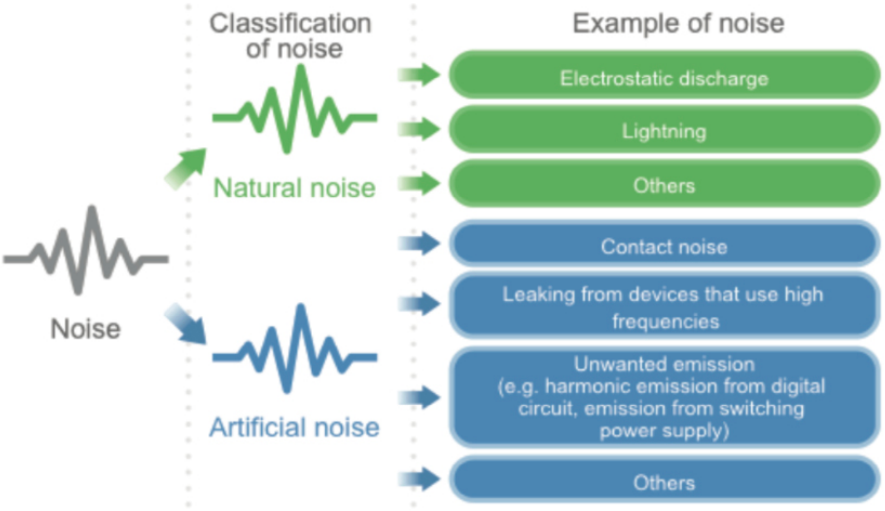

Figure 2. Classification of noise.

Source: Murata.com.

2.2.1. Analog circuit

From the viewpoint of noise source origin, analog circuits tend to generate relatively less noise since those only use limited frequencies and are designed to control the flow of electric current.

But still, if some of the energy leaks to the outside, it can be a cause of noise interference. For example, receivers for TV or radio use a signal with a constant frequency called local oscillator frequency in order to selectively amplify the targeted frequency from the radio waves that have been received by the antenna.

If this leaks to the outside, it can cause interference to other devices. In order to prevent this from happening, the tuner section is shielded or EMI suppression filter are used for the wiring.

In contrast, from the viewpoint of noise victim, since analog circuits often deal with faint signals and the information is affected by even small fluctuations, the circuit tends to easily become a noise victim. In order to prevent this fact, highly sensitive voice amplifiers are shielded or EMI suppression filters are used for the wiring.

2.2.2. Digital circuit

From the viewpoint of noise source origin, digital circuits are likely to become noise sources as the transition between the signal levels of 0 and 1 happens in a very short period of time, which contains an extremely wide range of frequency components. In order to prevent the noise emission, shields and EMI suppression filters are used for digital signals. Noise generated by digital circuits is an important topic, since it is not only related to signals but also related to power supply.

However, from the viewpoint of noise victim, the signals are expressed with only two statuses of 0 and 1 and have a relatively large amplitude. In addition, the information would not be affected by small induction. So, it is unlikely to become a noise victim. Nonetheless, if it gets high level noise even if it goes for a split second, the data will be completely altered. Therefore, it has a vulnerability to pulse noise such as an ESD (Electro-Static Discharge).

2.3. EMI shielding

EMI shielding is any method used to protect a sensitive signal from external electromagnetic signals, or preventing a stronger signal from leaking out and interfering with surrounding electronics.

The shielding can reduce the coupling of radio waves, electromagnetic fields, and electrostatic fields. A conductive enclosure used to block electrostatic fields is also known as a Faraday cage. The amount of reduction depends very much upon the material used, its thickness, the size of the shielded volume and the frequency of the fields of interest and the size, shape and orientation of holes in a shield to an incident electromagnetic field.

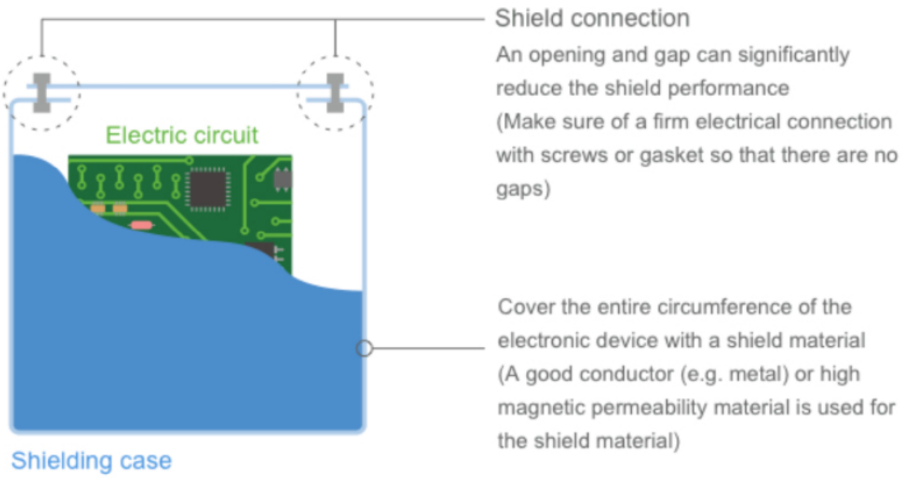

Figure 3. Enclosing an electric circuit with a metal plate.

Source: Murata.com.

As an example, Fig. 4 shows how the spatial noise conduction occurs inside an electronic device and how the noise is eventually emitted from the cable. These three mechanisms of spatial conduction are also applied to the case of noise conduction to the outside of the electronic device as well as to the case of noise reception. To block out the spatial noise conduction in the air, the target object should be shielded (Fig.4).

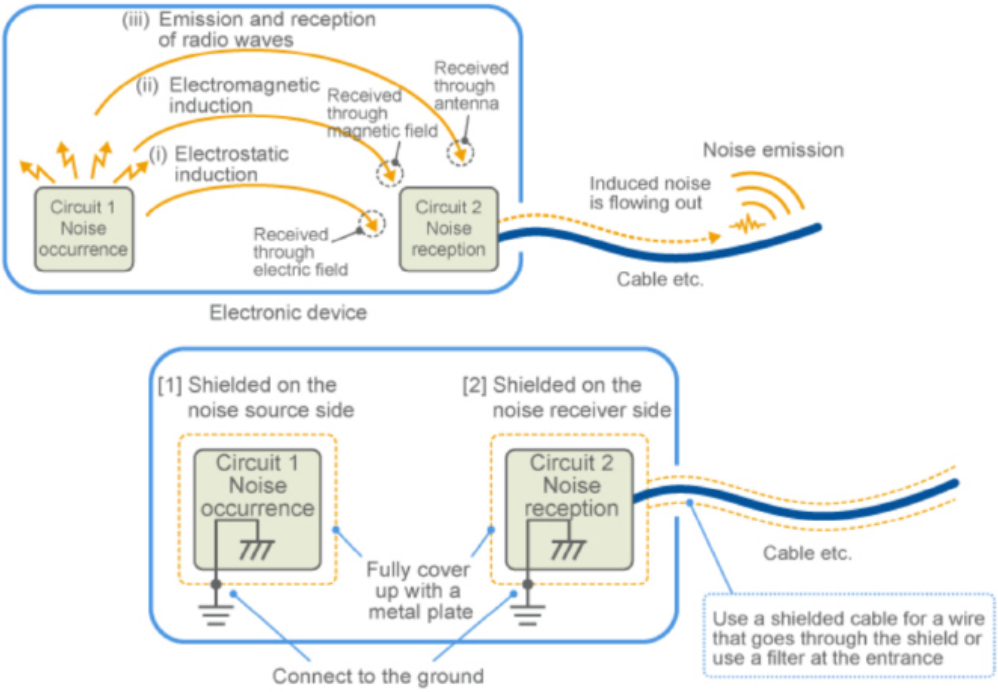

Figure 4. Effect of shield an electronic device.

Source: Murata.com.

Although the mind-set for shielding is slightly different depending on the noise induction model, the embodiment is almost the same. The reason is that even a thin metal foil can provide a sufficiently good effect in the frequency range of above several MHz unless it is under extreme conditions. In many cases, it requires ground connection and its effectiveness significantly varies depending on how good the ground is.

Nowadays, due to the ubiquitous presence of electronic circuits in all aspects of human lives, the study and modeling of EMC are more important than ever, especially in relation to extending these studies to the new frequencies that in a few years will be a reality in modern telecommunications systems, such as 5G (up to 27 GHz).

Currently, there exist several different approaches to mitigate the harmful effects of EM interferences, as illustrated in the following figure:

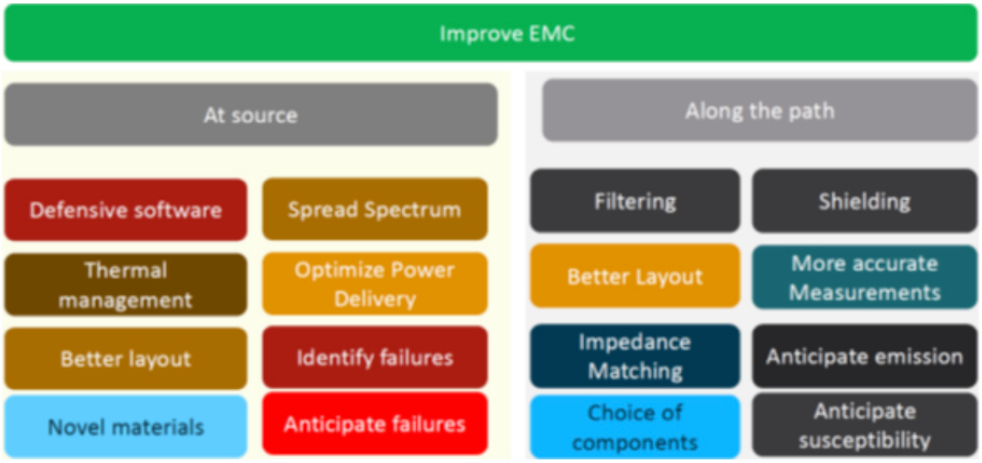

Figure 5. Possible solutions to mitigate EM interference effects.

Source: Google.com.

However, most of these solutions require anticipating the effect of EM interferences before designing and/or manufacturing the electronic device, and are not useful once it has been produced.

The ability to control complex EMI problems either by eliminating or by reducing them is in high demand [6]. Consequently, electromagnetic interference shielding (EMI Shielding) is one of the main concerns for electronic engineers, designing enclosures or devices that contain complex electronic systems [6]. EMI Shielding is defined as a certain method used in order to reduce electromagnetic field in a certain area.

EMI Shielding is focused on either protect susceptible devices against EM fields that can be present at the environment where they are going to work (increasing their immunity) or reducing the EM field produced by those devices that can generate a significant interference level (reducing their emissions). These two strategies of EMI Shielding are shown in Fig. 6.

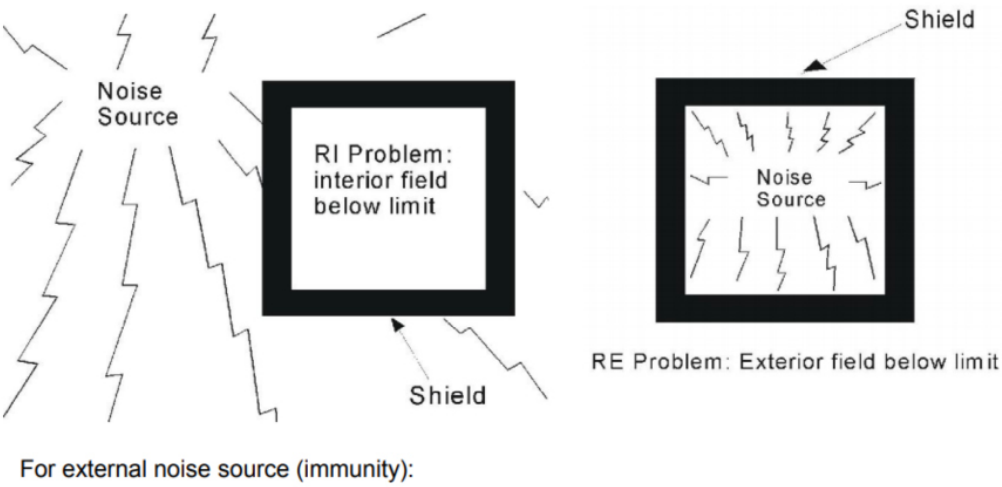

Figure 6. EM Shielding strategies: Increase the immunity (left), reduce emissions (right).

Source: Ott, H. W. (2011). Electromagnetic Compatibility Engineering.

Shields can be applied into a discrete component (i.e., a coil or integrated circuit (IC)) and, especially, interference area (i.e., a certain PCB track), a room (i.e., anechoic chamber) or a complete building (i.e., strategic buildings that are shielded against attacks through electromagnetic pulses (EMP)).

EMI Shielding is not only the most effective method against undesired EM fields, but also the unique method that makes it possible to improve the EMC of a system without reducing the working frequency of the devices that integrates it. Nevertheless, with the increase of the electronic components density in the system together with the increase of the operation frequency, EMI Shielding is essential to avoid the interferences between neighbor devices, areas of a same circuit or even between components. Nowadays, Design Engineers must create a PCB that provides the lowest possible EMI at the same time that it operates the fastest possible, reducing it as small as possible.

The Shielding techniques are widely used to get these last goals with the aim of adjusting the emission and immunity of electronic equipment to the limits imposed by the EMC standards. Other trending areas of interest covered by EMI Shielding solutions are the protection of data transmission and the protection of biological systems against EM fields in order to avoid potential risk to health [8][9].

The EMI Shielding products are an interesting tool both for Electronic Engineers and for Mechanical Engineers, since they offer the next advantages:

- EM Shielding products can be used as a ground reference, reducing the common mode coupling of the noise and the crosstalk undesired effect.
- They help to limit the electrostatic discharge (ESD), providing an alternative and safe low impedance path to the high current applied.
- They allow absorbing undesired electromagnetic energy through transforming it into heat.
- They are able to reduce cavity resonance problems in that circuits enclosed into a metal case.
- EM Shielding products improve the protection ability of a certain device or system against water, dust or any accidental contact (IP protection).

An ideal EMI Shield would be represented by a continuous conductive barrier with enough thickness and without openings that encloses an electronic device to provide insolation against EM fields. The ratio of the energy on one side of a certain Shield to the energy on the other of it is defined as Shielding Effectiveness (SE). This parameter is used to describe the ability of a Shield to isolate a device or system against EM fields. The SE can be produced by the ability of the Shield to reflect and absorb the EM fields.

One of the main Shielding methods used to protect an electronic device or system against EM fields is based on housing it into a metal case. However, often this solution it is not possible due to the system integrates openings in the casing (i.e., for cable inlets and outlets, ventilation slots, speakers…), it is an expensive solution, the weight or the volume of the device cannot be increased or the device has to be housed by a nonconductive enclosure [10].

Shielding techniques used to isolate certain devices against radiation in the far field are based on high conductive materials also known as “good conductors” such as aluminum or copper. This condition is achieved when the thickness of the Shield is much greater than a skin depth δ at the frequency of the incident wave.

The Shields constructed by “good conductors” materials are able to generate an

opposite field in the Shield surface due to the movement of the electrons when an incident field is applied. This induced field will mainly radiate in the opposite direction to the incident field, so the incident wave will be reflected as if it were a mirror. Due to the fact that the Shield is not a perfect conductor, the electrons located on the surface cannot move with the ease (conductivity of the material) and the velocity (frequency of the incident wave) necessary to compensate the whole incident field.

Thereby, a part of the incident field will penetrate the Shield and, at this point, it is important to consider the frequency of the radiation, the shielding material parameters and the skin depth. If the Shield is not thick enough, part of the incident field will cross the barrier passing to the other side of the Shield being present inside the protected area.

Therefore, if the shielding material and the thickness of the Shield are not selected properly it could be possible that the energy of the incident field was not totally reflected and absorbed and, thereby, the device to be isolated is partially irradiated. These mechanisms define the shielding effectiveness of a certain Shield to reflect or absorb undesired EM fields. Figure 4 shows a diagram that represents the different mechanism used by a certain Shield to attenuate an incident wave.

Thereby, the first shielding effect that takes place when a wave impact on a Shield is the reflection (R), since a portion of the incident wave is repelled by the surface. The part of the incident wave that is not reflected crosses the Shield, being attenuated according to the absorption (A) loss of the material. Subsequently, the part of the wave that is able to reach the other side of the Shield (right side in Fig. 7) represents the transmitted wave, referred to the part of the wave that the Shield has not be able to suppress.

There is a third mechanism related to the SE that is referred to the multiple internal reflections (M) produced inside the material. This last factor can be neglected if the material constitutes a “good conductor” (if A is higher than 6 dB, then M is not considered), considering only the initial reflection and transmission at the left and right interfaces of the Shield.

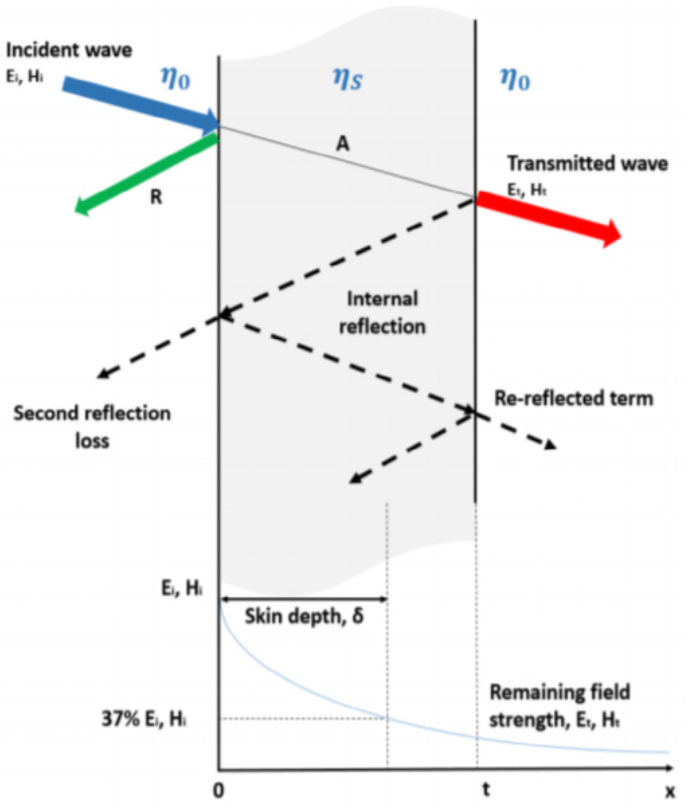

Figure 7. Attenuation of an electromagnetic wave by a shield.

Source: researchgate.net.

The Schelkunoff's SE approach [11] uses a basic model based on a transmission line connected to a generator and terminated at the other end with a defined impedance. Thereby, the voltage and current waves associated with the transmission line are replaced by the transverse EM fields by using Maxwell's equations. Therefore, the SE can be obtained through the Schelkunoff's approach through the sum of the three terms and it is expressed in decibels (dB):

Equation 1. Schelkunoff's SE approach.

$$SE = A + R + M$$

Source: [11].

Shielding theory is mainly focuses on far-field region, however, it is important to control the undesired EM fields in the near field region due to this is critical in dealing with Board Level Shielding (BLS). In the near field region, generally, it is more effective to reduce EMI by tackling it at the board level through shielding noisy parts and protecting sensitive circuits. Traditionally, one of the most used BLS techniques is based on enclosing an electronic circuit on a PCB with a faraday cage represented by a shielded metal can or cabinet.

However, the solutions related to attenuate EM interferences in the near field have increased in the last years, and other products such as ferrite sheets or flexible absorber sheets provide an innovative, thin and customizable solution in terms of BLS. It is very important to carry out a co-design during the hardware design process considering the use of EMI board level shields during the initial hardware design to take advantage, since it may eliminate the need of a shielding enclosure that covers the whole PCB instead of some parts of this. Therefore, this co-design can lead to a reduction in terms of cost and weight of the final certified product [12].

Therefore, the ideal electromagnetic shield is an infinitely conductive enclosure with no apertures or penetrations of any kind. Functional requirements and practicalities of design and construction prevent this ideal from being realized. Penetrations for power, signals, and ventilation as well as access apertures for calibrations, controls, and adjustments could be incorporated into an enclosure preventing it from being an ideal enclosure. An enclosure should include all of the intended design features when evaluating it for its shielding effectiveness.

Depending upon function and application, electronic equipment operates in an extremely wide range of electromagnetic environments in terms of both intensity and frequency. The environments can vary from that of the home to the battlefield. Because there is no “one size/type fits all” enclosure, the challenge facing equipment designers is that of choosing the most efficient and cost-effective shielding material for the particular enclosure intended for that particular application.

From this perspective, solutions based on metallic shielding are widely used by designers, because they allow mitigating the effects of EM interference that have not been foreseen in the design and/or manufacturing phases, and that could not be mitigated otherwise without having to redo the design and/or manufacturing processes.

Thereby, the conventional materials for EMI shielding based on metals possess a high density of mobile charge carriers, which blocks the EM waves mostly by the reflection mechanism. However, metallic shields are heavy and prone to oxidation, resulting in corrosion. Increase in temperature also leads to degradation of EMI shielding by metals. Furthermore, metal EMI shielding could not be effective for near field EMI generated by magnetic field couplings. In this situation, EMI shielding based on polymers with ferromagnetic embedded particles can provide a more significant performance.

2.3.1. Shielding and 5G technology

The 5G technology is having a significant impact on the communication industry since a great variety of innovative technologies are derived from it, such as Sub 6 GHz and millimeter wave (mmWave) in the 28 GHz spectrum. This new technology provides high communication speeds and low latency. Furthermore, the SiP (System in Package) design and assembly technology play a key role in the IoT (Internet of Things) field. Due to this technology's properties, the influence of electromagnetic interference on other equipment and systems is a line of research with excellent projection.

The current situation is finally at a state where actual 5G devices have started to appear, but because it takes time to evaluate using actual devices, envisioning a system where a millimeter wave circuit like that shown in the Fig. 8, was added to a 5G communication circuit. Then, it is used a frequency multiplier and mixer test boards installed in the circuit to evaluate the effect when external noise connects to a signal line required for operation.

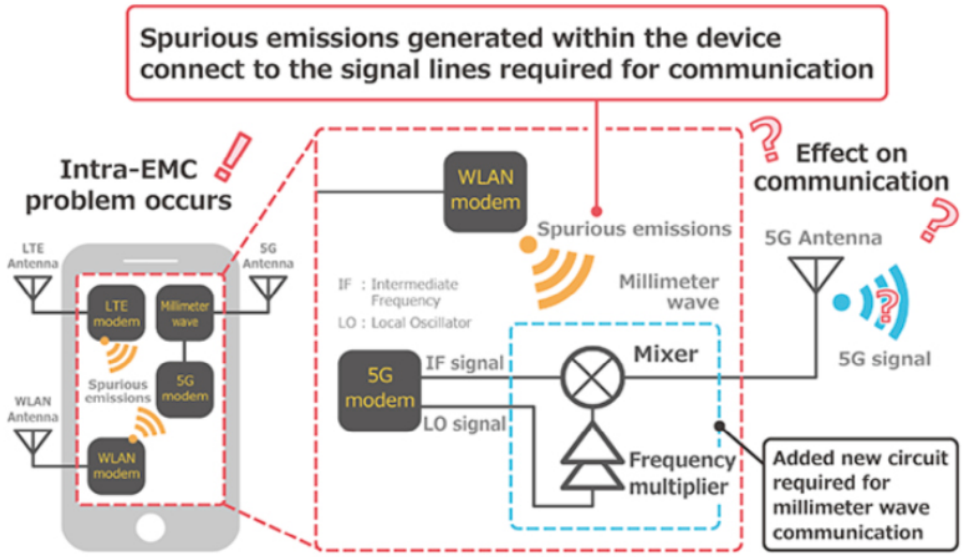

Figure 8. EMI effect when external noise connects to a signal line.

Source: Murata.com.

One of the 5G challenges is the design of new EMI shielding techniques that allow 5G to coexist with other technologies. In this way, it is necessary to develop EMI shielding materials that ensure compliance with the different standards that regulate 5G and the proper operation of possible systems susceptible to the intentional and unintended signals generated by this new technology.

The 5G spectrum is divided into two regions, FR1 and FR2.

- The frequency range 1 is from 410 MHz up to 7125 MHz, and its also called Sub-6 GHZ band.
- The frequency range 2 its up to 52 GHz. Most of the electromagnetic wave wavelengths in this spectrum are in the millimeter level, so it is also called mmWave.

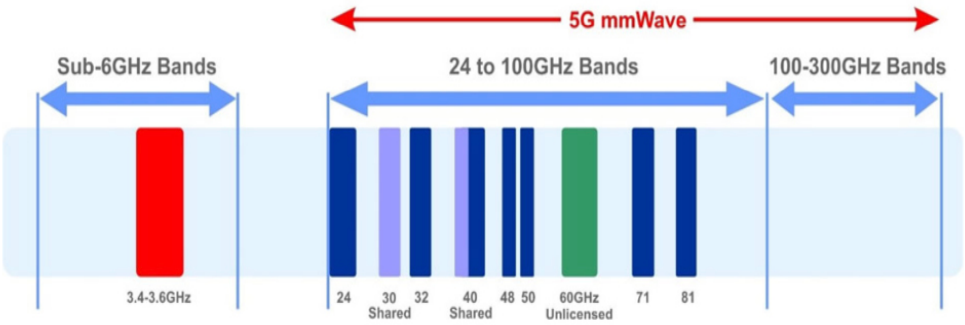

Figure 9. mmWave Frequency Bandwidth.

Source: spectrumfutures.org.

With the emergence of 5G communications, it is a need to design new EMI shielding materials and techniques in the direction of higher shielding effectiveness, wider shielding frequency, and better performance. The use of traditional shielding techniques, such as metal shielding, can be effective to attenuate EMI generated by 5G applications but have some drawbacks, such as high weight and volume.

This is why other solutions based on polymers, plastic materials, and even fabrics are being studied to provide the necessary shielding effectiveness at the same time that offers lower weight and volume. An example of a shielding polymer is the use of carbon nanofibers (CNF) to achieve a material with optimal shielding properties and reduced weight and volume [13].

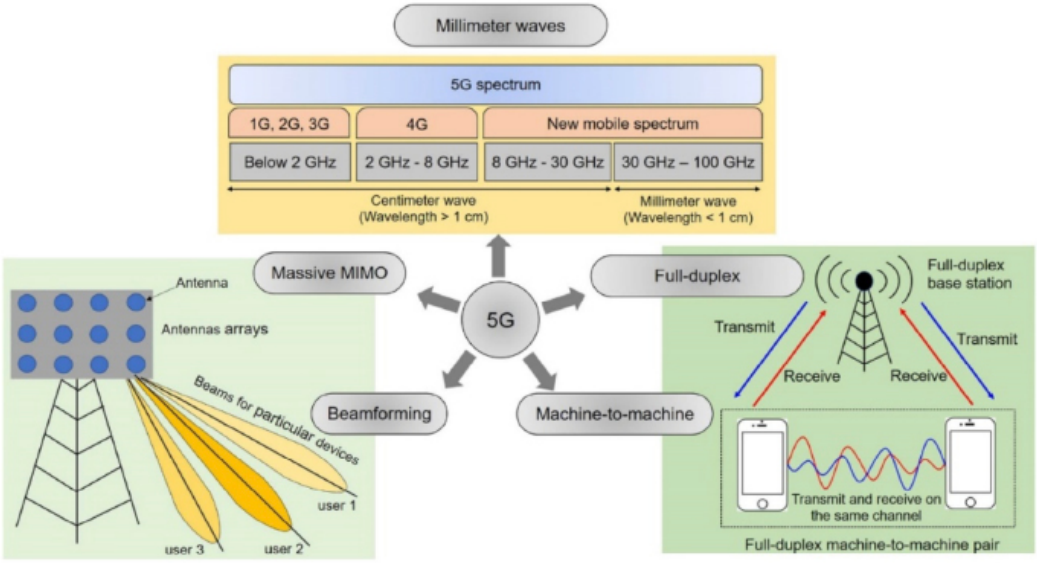

Figure 10. Advanced technologies that include mmWaves.

Source: degruyter.com.

Another example of techniques to obtain shielding materials for 5G is the use of composites formed by nanotubes, making it possible to create lightweight materials able to replace the traditional metallic materials. Furthermore, due to their plastic properties, these materials are easily adaptable to our systems, providing numerous advantages over metallic materials that are rigid and, therefore, are not easily adaptable to different systems [14][15][16]. Consequently, new optimized materials must be designed to meet 5G technology requirements while ensuring the proper operation of new systems sensitive to these signals, such as electric vehicles, chargers, or more compact communication systems.

Metals or metal alloys, such as copper, aluminum, stainless steel, etc. are the most common materials for EMI shielding. As conventional shielding materials, metals demonstrate adequate shielding capacity against EMI. However, polymers have become up-and-coming materials for EMI shielding with the characteristics of lightweight, flexibility, cost-effective, easy processing, and resistance to corrosion.

It is true that plastic materials not present the best shielding properties front electromagnetic interference, but it is true too that with them it is possible to enhance the efficiency of automotive sector. The use of plastic materials or conductive

composite plastics allow this sector to cut both cost and emission because of their light weigh, reducing the total weigh of the vehicle is possible to extend its life cycle too, as making more efficient this industry.

The introduction of polymer composites against metal materials let save significant weight to the vehicle. With lightweight materials in vehicles improve safety, environmentally friendly through material savings, reduced fuel consumption and CO2 emissions. A lightweight of 10% in the vehicle let optimize energy consumption between 6-8% improving battery autonomy. The use of more plastic body work will increase the driving range and more fuel-efficient and thus friendlier to the environment. At the final life cycle, it is possible the use of waste plastics as a means to generate and recover energy.

The vehicle of the future, with the introduction of Advanced Driver Assistance Systems (ADAS) and other semi-autonomous driving technologies, will be a media center as an extension of the office and home's living room while also the vehicle moves from point A to point B. The huge number of electronics systems in new vehicles and this, in turn, will dramatically extend the demands on the EMI shielding devices used to attenuate the radiated emissions that could affect circuits in the car. EMI shielding materials will need to perform over a wide range of frequencies, in more applications as electronic systems take over more and more aspects of the car's driving operations while adding as little as possible to the weight of the vehicle [17][18].

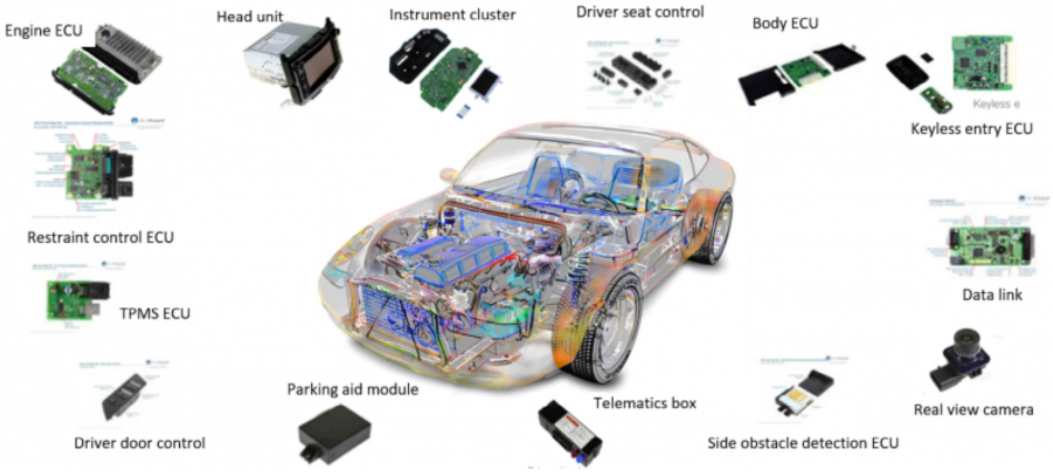

Figure 11. EMC in different electronic modules of a vehicle.

Source: silvaco.com.

Tom Wenzel of Lawrence Berkeley National Laboratory (LBNL), found the reductions in vehicle mass recommended by the 2015 National Academy of Science fuel economy subcommittee report (reduce the mass of small cars by 5%, midsize cars 10%, large cars 15%, and light trucks, CUVs, and minivans 20%) would result in even larger net reductions in fatalities than EPA's 100-lb or comparable proportional reduction in mass across all types of light-duty vehicles.

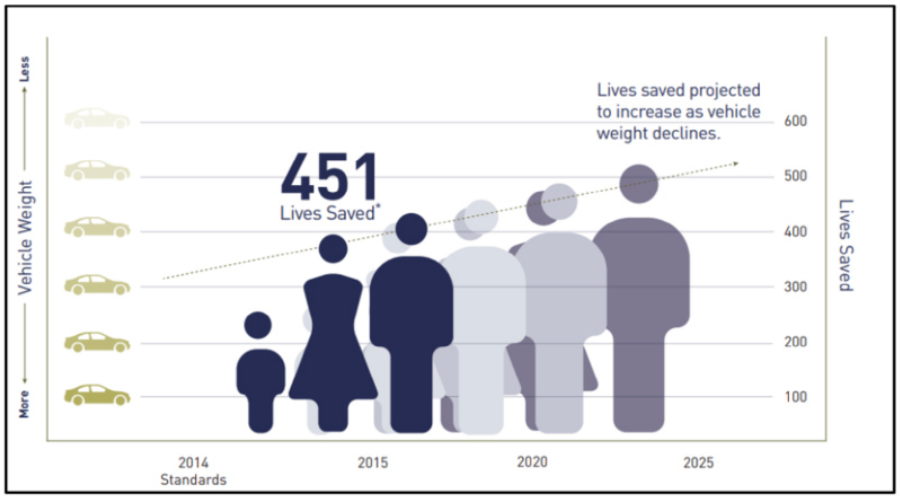

Figure 12. Estimation of lives saved as vehicle weight declines.

Source: automotiveplastics.com.

Ferromagnetic metal materials are also used in EMI shielding for their high initial permeability and low coercivity (ability of a ferroelectric material to withstand an external electric field without becoming depolarized). Ferromagnetic materials used for EMI shielding include iron, silicon-iron, Fe-Al alloy and perm alloy. One of the most used materials for shielding enclosures is Mu-Metal ® which is an alloy composed of 14 % iron, 5% copper, 1.5 % chromium and 79.5 % nickel. This material has high relative permeability between 80000 – 100000 and is considered a soft ferromagnetic material.

In recent years, the carbon-based materials with high EMI shielding performance have attracted intensive attention due to their comprehensive advantages over conventional metal-based EMI shielding materials ¡Error! No se encuentra el origen de la referencia.. In general, there are mainly three design strategies for carbon-based EMI shielding materials [20]. The primary is using conductive carbon materials

or composite materials that containing conductive carbon networks to reflect microwaves based on the principle of impedance mismatch [21][22].

Typically, the carbon-based nanotubes (CNTs) [23][24], graphene oxide (GO) [25] [26], and metal carbides nitrides (MXenes) [27] composite materials have been extensively reported and gained rapid development in recent years. Their superior electrical conductivity is beneficial to construct continuous conductive network and thus enhancing the EMI shielding performance.

A recent work, reported on the scalable synthesis of composites with graphene fillers, and testing their EMI shielding efficiency in the X-band (frequency range of 8.2 GHz – 12.4 GHz) and the extremely high frequency (EHF) band (frequency range of 220 GHz – 325 GHz) [28]. The examined frequency bands are pertinent to state-of-the-art and future communication systems.

It was found that the composites of 1 mm thickness with graphene loading of only 8 wt% provide excellent electromagnetic shielding of 70 dB in the sub-terahertz EHF frequency with negligible energy reflection to the environment. The 70-dB shielding corresponds to blocking 99.99999% of EM energy.

In the X-band frequency band, graphene composites have also been tested for performance at elevated temperatures, demonstrating properties superior to other composites with conductive metal fillers.

Li J. et al [29] investigated the CCF@CoFe/PI composite films showing favorable flexibility and mechanical strength of 9~11 MPa at tensile break, as well as superb EMI shielding performance of ~32 dB over the X-band with the thickness of only 0.16 mm, and the EMI shielding efficiency of ~62 dB was achieved by stacking 6 layers of CCCF-800-2 films with the thickness of less than 1 mm. Moreover, the electromagnetic property of CCF can be adjusted by changing the CoFe content or carbonization temperatures, and the prepared CCF@CoFe/PI films hold great potential for large-scale applications in the flexible microelectronics and novel telecommunication equipment.

El Kamchi et al studied a multi-layered structure with PANI and PU where carbon coated cobalt (CCo) and FeNi nanoparticles were dispersed [30]. It was achieved an excellent SE of 90 dB over an 8- 18 GHz band frequency.

Ferrites, belonging to ferromagnetic material, they are economic for a wide range of applications and ease of fabrication into complex shapes. Thus, the use of hybrid ferrites fillers based on various combinations will be a possible solution for improved shielding effectiveness as well as the mechanical properties of nanocomposites [31]. As reviewed, different studies showed EMI shielding properties of carbon base and metallic polymer composites for low frequencies (below 3 GHz).

These composite materials are potential materials for 5G shielding due to their unique electromagnetic properties and outstanding thermal conductivity and strength, but it should be investigated for higher frequencies (on millimeter waves of 30–100 GHz).

2.4. Conclusions

This chapter has covered the basic EMC theory necessary to understand and contextualize the project. It has also discussed electromagnetic noise and EMI, which are the main problems to be treated using the materials proposed in this project. On the other hand, the theory of EMI shielding and the importance of this issue concerning 5G was introduced.

With all these facts, it has given way to the "shielding and 5G" section, where this new technology is introduced, the operating frequency ranges, and how this technology affects the current situation. Finally, EVA's and the future of 5G are discussed, justifying the objectives set for this project in section 1.2.

Chapter III: SHIELDING COMPOSITE STRUCTURES

3.1. Selection of materials for the study

By definition, a composite is a multiphase material formed from a combination of materials which differ in composition or form, retain their own chemical and physical properties, and maintain an interface between components which act in concert to provide improved specific or synergistic characteristics not obtainable by any of the original components acting alone [32][33][34].

Any composite is composed of almost two categories of materials: the reinforcement or filler and the matrix. The reinforcements contribute useful properties (mechanical, electrical, thermal, optical, etc.) to enhance the matrix properties.

In this case, for the development of composites with electromagnetic shielding properties, three different types of materials have been selected. First, an epoxy matrix that is reinforced with fiber fabric layers, and three conductive materials. And then, these structures are combined with a conductive material to improve the shielding effectiveness of the different structures.

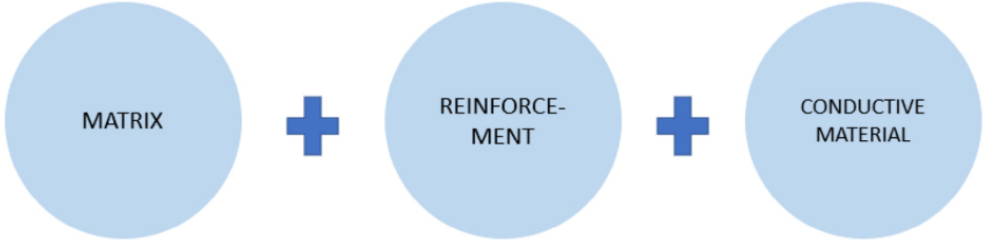

Figure 13. Schematic of the development of the composite materials.

Source: own elaboration.

Table 1 summarizes materials used to manufacture the eight composite samples evaluated in this contribution.

Table 1. Materials used to make the eight composite samples.

Material type	Description
Matrix	Cycloaliphatic epoxy resin system
Reinforcement	Biaxial carbon fiber fabric
Reinforcement	Biaxial glass fiber fabric
Conductive	Copper
Conductive	MW-CNT
Conductive	Graphite-Nickel

Source: own elaboration.

Two different fibers fabric are used as reinforcement in order to evaluate its contribution in terms of SE. This structure is combined with a conductive material with the aim of improve the SE. The conductive materials analyzed corresponds to a copper (Cu) mesh layer, a Multi-Walled carbon nanotubes (MW-CNT) layer and a nickel coated graphite layer.

Carbon nanotubes (CNTs) are tubes made of carbon with diameters typically measured in nanometers. Although not made this way, single-wall carbon nanotubes can be idealized as cut-outs from a two-dimensional hexagonal lattice of carbon atoms rolled up along one of the Bravais lattice vectors of the hexagonal lattice to form a hollow cylinder.

In this construction, periodic boundary conditions are imposed over the length of this roll up vector to yield a helical lattice of seamlessly bonded carbon atoms on the cylinder surface.

Carbon nanotubes also often refer to multi-wall carbon nanotubes (MW-CNTs) consisting of nested single-wall carbon nanotubes weakly bound together by van der Waals interactions in a tree ring-like structure [35]. If not identical, these tubes are very similar to Oberlin, Endo, and Koyama's long straight and parallel carbon layers cylindrically arranged around a hollow tube. Multi-wall carbon nanotubes are also sometimes used to refer to double- and triple-wall carbon nanotubes (Fig. 14).

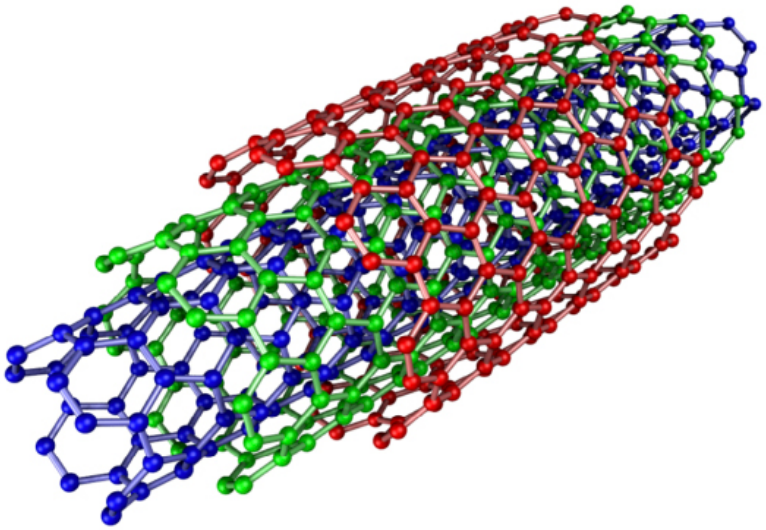

Figure 14. Triple-walled armchair carbon nanotube.

Source: en.wikipedia.org.

The introduction of CNTs inside host polymeric matrices leads to improvement of electrical conductivity as well as real- and imaginary-permittivity values [36][37]. These are direct manifestations of increase in number of conducting links and interfacial polarization phenomenon and lead to improvement in SE

On the other hand, the selected reinforcements and conductive materials employed for the manufacturing of composites with EMI shielding properties are shown in Fig. 15. The biaxial carbon fiber fabric and biaxial glass fiber fabric selected as reinforcements are shown in Fig. 15(a) and Fig. 15(b), respectively. The selected conductive materials are shown in Fig. 16(a)–(c)).

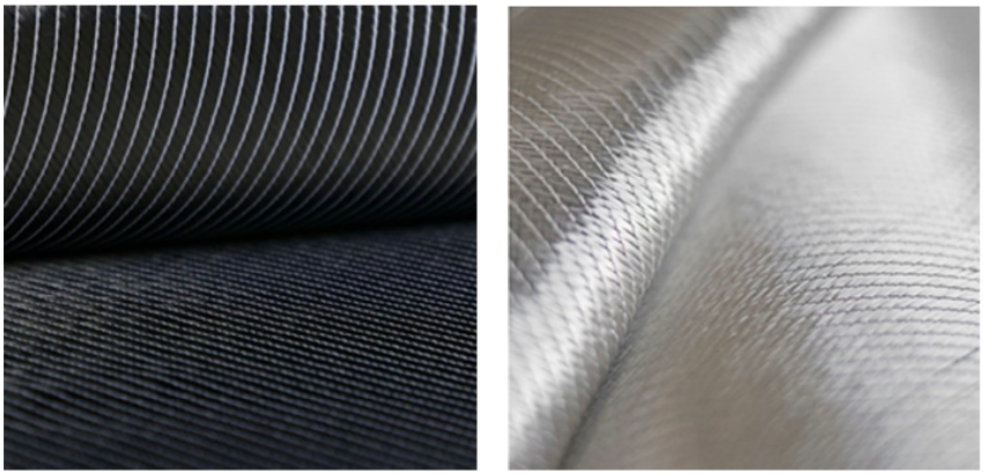

(a) (b)

Figure 15. Biaxial carbon fiber fabric (a), Biaxial glass fiber fabric (b).

Source: own elaboration.

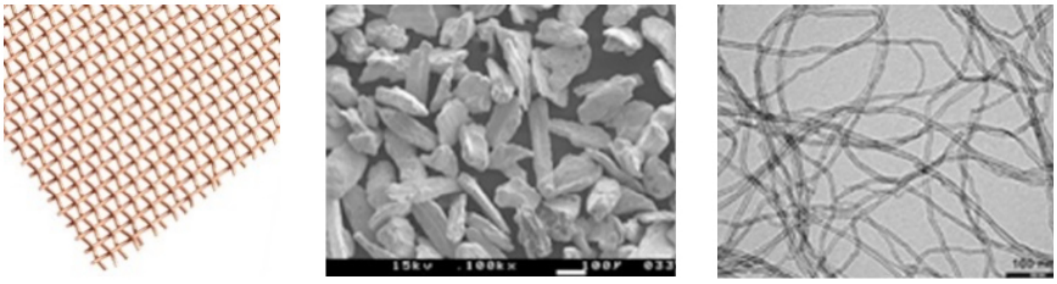

(a) (b) (c)

Figure 16. Conductive materials. (a) Copper mesh. (b) Graphite-Nickel. (c) MW-CNT.

Source: own elaboration.

3.2. Manufacturing process and resulting materials

Composite laminates have been manufactured by hand lay-up and vacuum bagging process. Hand lay-up is the simplest composite manufacturing method as shown in Fig. 17. The methodology consists in place the reinforcement layers on the mould and impregnate them manually with the thermosetting resin. Consolidation rollers

are used to thoroughly wetting the reinforcement and removing entrapped air. Subsequent layers of reinforcement are added and impregnated to build laminate thickness.

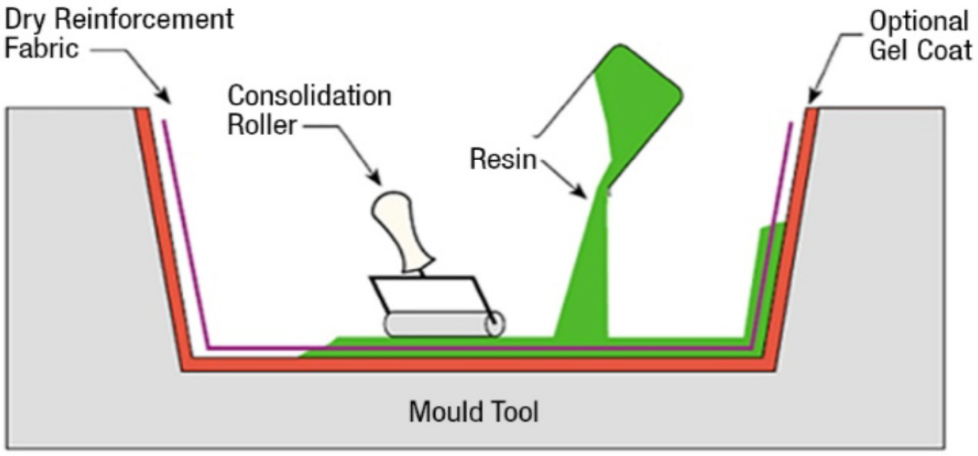

Figure 17. Hand lay-up composite manufacturing process.

Source: nexusprojects.com.

Vacuum bagging is applied to consolidate the composite laminate as shown in Fig. 18. After hand lay-up, the uncured laminate is covered with a peel ply (a synthetic fabric with a fine weave that assists with demoulding and surface finish), a release film (a perforated film that helps to evacuate entrapped air uniformly, while evacuate any resin excess that bleeds out of the composite) and a breather fabric (a relatively thick non-woven fabric that absorbs the resin that passes through the release film).

After this, the entire lay-up is then covered with a vacuum bag and sealed around the edges, apart from the connection to the vacuum pump. Activating the pump sucks all the air out of the space between the vacuum bag and the mould, causing the composite to be consolidated under 1 bar of pressure and at room temperature. Once the part is fully cured, the vacuum pump can be disconnected, the vacuum bag, breather fabric, release film and peel ply removed and discarded, and the part removed from the mould.

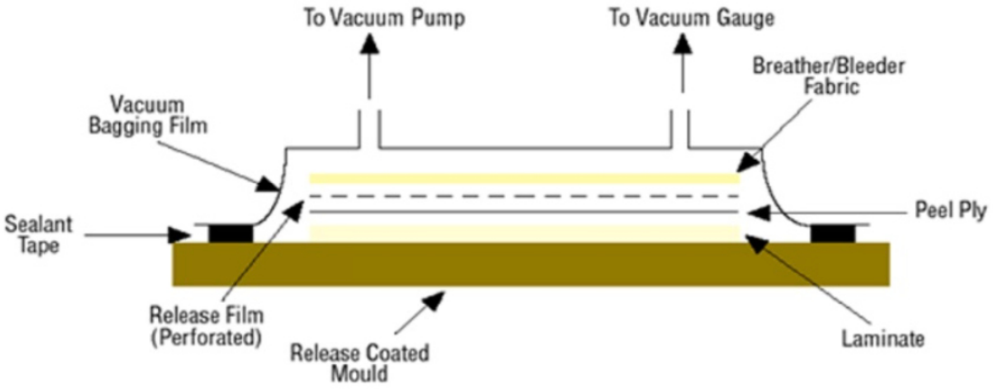

Figure 18. Hand lay-up composite manufacturing process.

Source: nexusprojects.com.

Within this processing methodology, the selected conductive materials have been included to their respective composite laminates following different methods:

- MW-CNT: Dispersion of nanoparticles in the matrix using a high-speed dispersing equipment. The mix has been used in the impregnation of all reinforcement layers of the composite laminates.
- Graphite-Nickel: Manual mixing in the matrix. The mix has been applied between layer 3 and 4 of the composite laminates.
- Cooper mesh: Placement of the mesh between layer 3 and 4 of the composite laminates, obtaining a sandwich structure.

Following the different described methodologies, eight composite laminates have been obtained. Their composition and thicknesses are summarized in Table 2:

Table 2. Composition and thicknesses of composite laminates.

Reference	Reinforcement	Conductive material	Thickness (mm)
CF	6 x Carbon Fiber	-	2.30
CF + Cu	6 x Carbon Fiber	Copper	2.45
CF + MW-CNT	6 x Carbon Fiber	MW-CNT	2.30
CF + Gr-Ni	6 x Carbon Fiber	Graphite-Nickel	2.45
GF	6 x Glass Fiber	-	2.31

GF + Cu	6 x Glass Fiber	Copper	2.45
GF + MW-CNT	6 x Glass Fiber	MW-CNT	2.26
GF + Gr-Ni	6 x Glass Fiber	Graphite-Nickel	2.62

Source: own elaboration.

Finally, these composite laminates have been machined using a CNC (Computer Numerical Control) machining equipment to obtain specimens with the appropriate dimensions for subsequent analysis. Fig. 19 shows an example of the specimens obtained after the machining tasks.

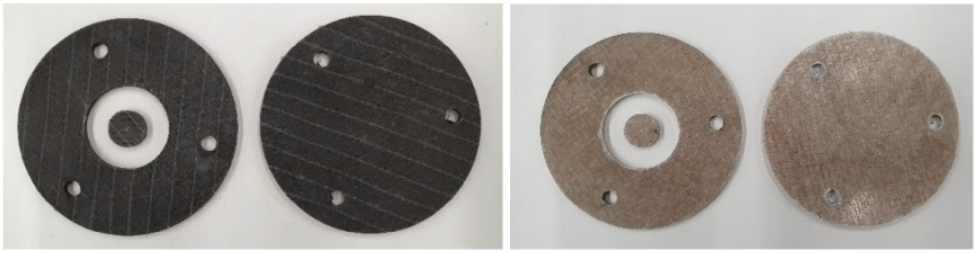

(a) (b)

Figure 19. Example of machined composite specimens for the EMI shielding test. (a) Carbon fiber. (b) Glass fiber.

Source: own elaboration.

3.3. Conclusions

This chapter has focused on the objective set in section 1.2. Study, design, and manufacture new plastic materials with EM shielding properties in the 5G frequency range. The eight main materials measured in this research have been presented. It has been explained in general terms the composition of each of the samples and the three conductive materials that have been selected.

The manufacturing process of the composite structures has also been briefly presented, to finish with the final result of the test samples.

CHAPTER IV: MEASUREMENT SETUP

4.1. Introduction to the method

There are multiple methods to measure electromagnetic shielding, but one of the most widely accepted is the ASTM 4935-18 standard.

As for frequency range limitations, this method allows measuring planar samples in a narrow frequency range from 30 MHz to 1.5 GHz. These limits are based on the decrease in current displacement due to capacitive coupling at very low frequencies and overmodulation at higher frequencies where the wavelength is comparable to the size of the sample used in this method [38].

The method consists on the measurement of the insertion loss (IL) that results when introducing test samples in a coaxial two-conductor transmission line holder, supporting transverse electromagnetic (TEM) propagation mode (Fig. 20).

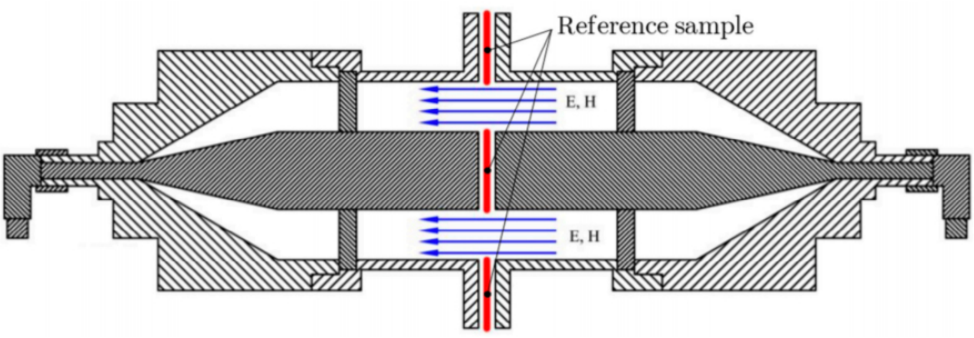

Figure 20. Cross Section of sample holder according to ASTM 4935-18.

Source: [38].

To obtain the measurements, it has been decided to use a Vector Network Analyzer (VNA), more specifically the Keysight E7051B, which allows measurements from 300 kHz to 8.5 GHz (Fig. 21). It also has a dynamic range of 125 dB, which is sufficient to measure the SE of the selected materials, and four Type-N female connectors with a characteristic impedance of 50 Ω [39].

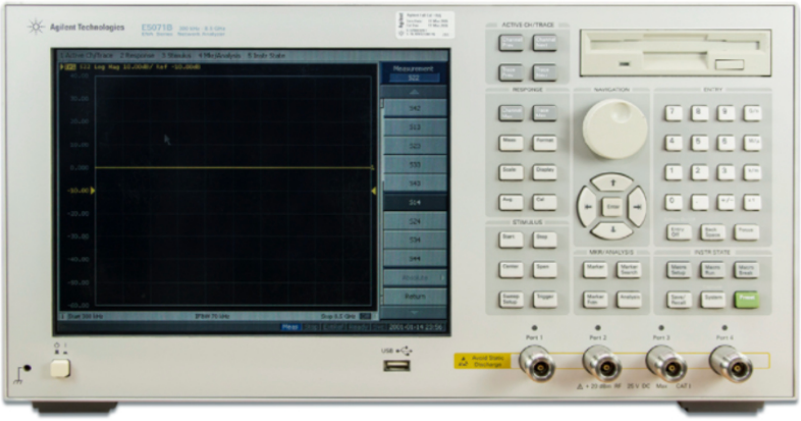

Figure 21. VNA Keysight E5071B

Source: own elaboration.

The specimen holder is a coaxial transmission line with special taper sections and notched matching grooves to maintain a characteristic impedance of 50 Ω throughout the entire length of the holder as shown in Fig. 22.

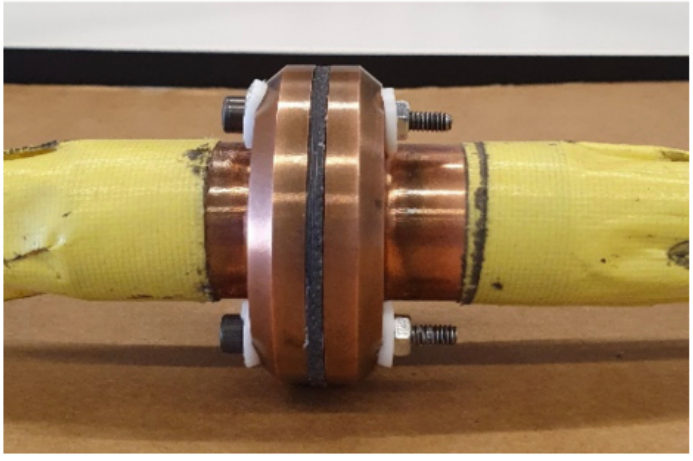

Figure 22. Coaxial transmission line holder with a test sample introduced.

Source: own elaboration.

The procedure requires two types of specimens that must have the same thickness in order to make SE measurements, the reference and the load specimens. The thickness of the tested materials cannot exceed 1/100 of the wavelength of the EM

wave in open space, i.e., the thickness of the material should not exceed 2 mm for a test frequency of 1500 MHz or 3mm for 1000 MHz.

The difference between the measurements of the load and the reference specimen provides the measurement of the SE, caused by the reflection and absorption of the material between the two flanks of the coaxial probe.

The use of two different specimens is justified by the fact that the use of the reference specimen can compensate the effects of capacitive coupling by establishing a frequency-dependent reference level [20][21].

The load specimen has a disk-like shape with diameter equal to that of the outer flange. On the other hand, the reference specimen consists of two parts: a washer and a disk-shaped sample, matching the dimensions of the outer and inner conductors, respectively.

Fig. 23 shows the measurement setup described previously and the dimensions of the specimens, both the reference and the load.

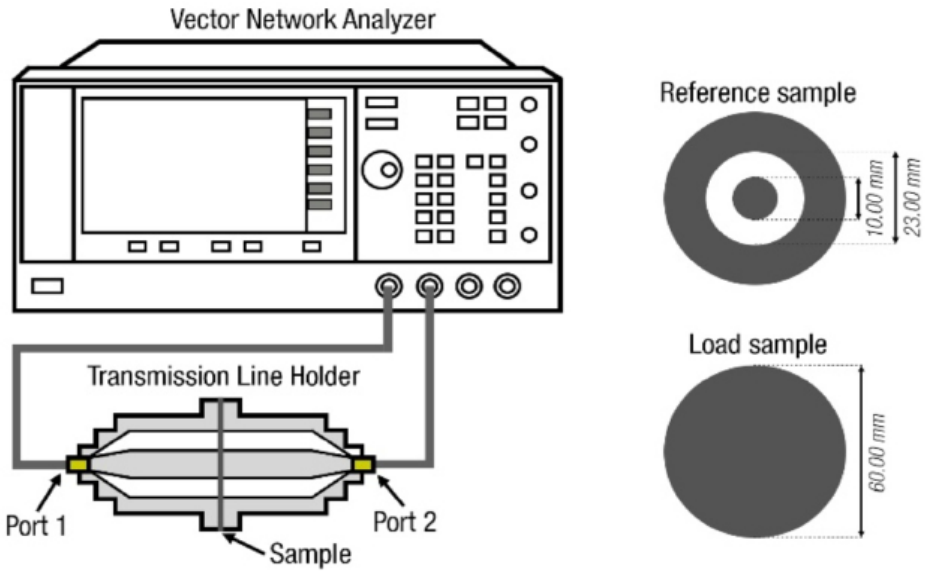

Figure 23. Schematic of measurement test setup following the ASTM D4935-18 procedure.

Fuente: own elaboration.

Fig. 24 shows the experimental setup implemented to characterize the samples

under test with the VNA E5071B and the transmission line holder according to the ASTM 4935-18 standard.

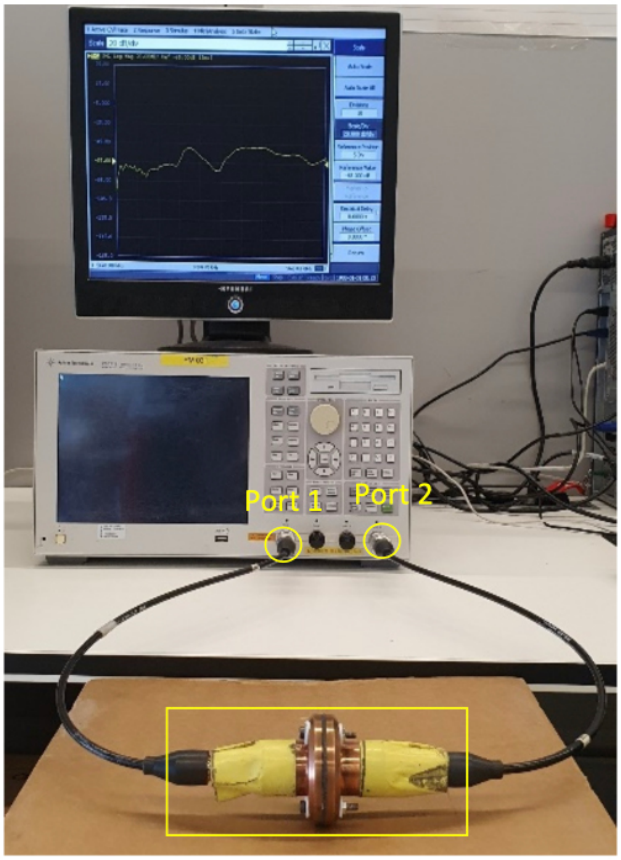

Figure 24. Measurement test setup following the ASTM D4935-18 procedure.

Fuente: own elaboration.

To perform the measurements, the network analyzer has been configured in a specific way. First of all, the "SMOOTH" has been activated for all measurements. In this way, the traces are much cleaner than without this option activated.

On the other hand, the "SWEEP SETUP" has been configured with a "LINEAR SWEEP" and a number of points of 1201. This number of points is sufficient to display the trace with enough resolution.

As for the display format, "LOG-MAG" (logarithm-magnitude) has been selected. The measurement mode in the "MEASUREMENT" field is S21 and, in the "STIMULUS"

submenu, the frequency range is selected. In this case, the start frequency is the minimum frequency of the equipment (300 kHz) and the stop frequency is the maximum (8.5 GHz). Thus, measurements are performed over the entire bandwidth of the equipment.

4.2. Measurement principle

The shielding effectiveness (SE) is typically defined as the ratio of the magnitude of the incident electric field, to the magnitude of the transmitted electric field.

There are several factors that determine de SE:

- Frequency of the electromagnetic field.
- Shield material parameters (conductivity, permeability and permittivity).
- Shield thickness.
- Type of electromagnetic field source (plane wave, electric field, or magnetic field).
- Distance from the source to the shield.
- Shielding degradation caused by any shield apertures and penetrations
- Quality of the bond between metal shield surfaces.

On the other hand, the insertion loss (IL) is the loss of signal power resulting from the insertion of a device in a transmission line. In this way, the SE measurement (dB) can be expressed as the difference between the IL expressed in dB of the load specimen ($IL_{dB,l}$ and the IL of the reference one ($IL_{dB,r}$):

Equation 1. Shielding effectiveness in terms of insertion loss.

$$SE_{dB} = IL_{dB,l} - IL_{dB,r}$$

Source: ASTM 4935 Standard.

The $IL_{dB,l}$ and $IL_{dB,r}$ measurements can be done directly from the VNA due to the measurement method used, by placing the probe terminals between ports 1 and 2 of the network analyzer and selecting the measurement of complex scattering parameters (or S-parameters), specifically, the S21, both for the reference and for

the load. Therefore, SE_{dB} can be expressed as:

Equation 1. Shielding effectiveness in terms of S_{21}.

$$SE_{dB} = 20 \log_{10} \left| \frac{S_{21,l}}{S_{21,r}} \right|$$

Source: ASTM 4935 Standard.

Whereas the frequency range established by the ASTM 4935-18 standard is limited to frequencies below 1.5 GHz, measures have been carried out from 300 kHz to 8.5 GHz, to observe the tendency of the behavior of the different materials in the FR1 frequency range (410 MHz – 7125 MHz) [40].

Apart from the measurements performed with the VNA E5071B, preliminary measurements were also carried out with the VNA 8753ES (Fig. 25). The frequency range is from 30 kHz up to 3 GHz. This is a rather low bandwidth compared to the VNA E5071B. It also has only two ports with 7mm type connectors.

Figure 25. VNA 8753ES.

Source: own elaboration.

The comparison of the measurement of the CF + MW-CNT composition sample is shown in Fig. 26, where the difference between the two measurements can be clearly seen. The VNA E5071B shows a much cleaner and stable trace (red trace), while the grey trace representing the measurement with the 8753ES, presents oscillations and peaks that make the accuracy of the measurement more variable.

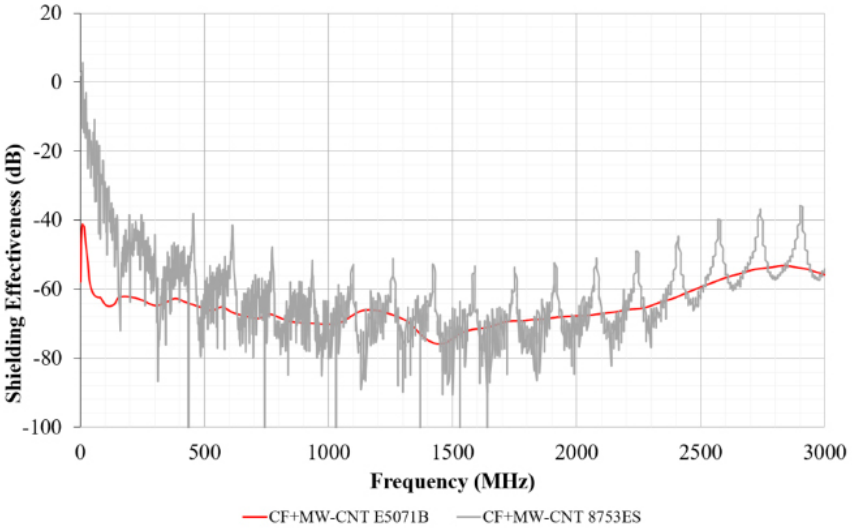

Figure 26. Comparison between measurements of the two different VNAs.

Source: own elaboration.

Since these measurements are usually given in terms of frequency, i.e., -56dB @ 500MHz, the trace must be kept clean and smooth.

With the oscillations of the trace corresponding to the VNA 8753ES, an error over 10dB of the SE value for a given frequency can occur. After these preliminary tests and measurements, it was decided to perform the measurements with the E5071B.

4.3. Data treatment

Once chosen the VNA with which the measurements are going to be performed, and the principle on which they are based has been explained, the data treatment process followed will be briefly explained.

Once the desired graph is obtained on the screen of the VNA E5071B, the data has to be export following the next sequence of clicks: Save/Recall → Save Trace Data (Fig. 27).

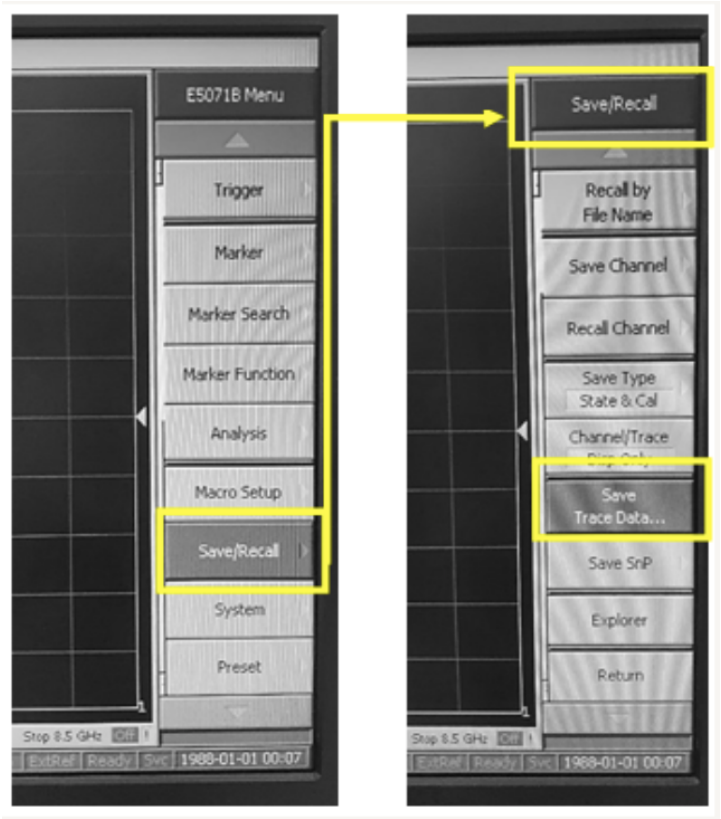

Figure 27. Save the data file. (a) Save/Recall. (b) Save Trace Data.

Source: own elaboration.

Then, the file is named with the reference of the sample that is being measured and whether it is the reference sample or the load. The file is saved automatically in ".csv" format. In this excel file it can be seen the configuration of the VNA, and the raw data obtained from the measurement. An example of the file obtained directly from the VNA is shown in the Fig. 28.

	A	B
1	Trace	
2	Swept SA	
3	A.14.62	N9010A
4	503 B25 EP3 P03	1
5	Segment	0
6	Number of Points	1001
7	Sweep Time	0.0028
8	Start Frequency	300000
9	Stop Frequency	3000000000
10	Average Count	100
11	Average Type	LogPower(Video)
12	RBW	1000000
13	RBW Filter	Gaussian
14	RBW Filter BW	3dB
15	VBW	50000000
16	Sweep Type	Swept
17	X Axis Scale	Lin
18	PreAmp State	On
19	PreAmp Band	Low
20	Trigger Source	Free
21	Trigger Level	1.2
22	Trigger Slope	Positive
23	Trigger Delay	0
24	Phase Noise Optim	Fast
25	Swept If Gain	Low
26	FFT If Gain	Autorange
27	RF Coupling	AC
28	FFT Width	411900
29	Ext Ref	10000000
30	Input	RF
31	RF Calibrator	Off
32	Attenuation	0
33	Ref Level Offset	0
34	External Gain	0
35	Trace Type	Maxhold
36	Detector	Peak
37	Trace Math	Off
38	Trace Math Oper1	Trace5
39	Trace Math Oper2	Trace6
40	Trace Math Offset	0
41	Normalize	Off
42	Trace Name	Trace1
43	X Axis Units	Hz
44	Y Axis Units	dBm
45	DATA	
46	300000	-32.9705925
47	3299700	-55.74814224

Figure 28. File with ".csv" extension.

Source: own elaboration.

In order to be able to represent the measurements and their interpretation, it was necessary to re-format the data and perform the operation as explained above in Eq. 2 to obtain the SE. Furthermore, to make the representation easy to interpret, it was decided to represent the abscissa (x) axis in MHz. An example of the formatted ".xlsx" file is shown in the Fig. 29.

Frequency (Hz)	Frequency (MHz)	(IL) Reference	IL (Load)	SE (dB)
300000.00	0.30	0.42	=D4:D1604-C4:C1604	
2170000.00	2.17	0.04	-65.11	-65.16
4050000.00	4.05	-0.03	-64.99	-64.96
5920000.00	5.92	-0.03	-64.81	-64.78
7800000.00	7.80	-0.04	-64.92	-64.88
9670000.00	9.67	-0.04	-65.08	-65.04
11500000.00	11.50	-0.05	-65.12	-65.07
13400000.00	13.40	-0.05	-65.23	-65.18
15300000.00	15.30	-0.05	-65.43	-65.38
17200000.00	17.20	-0.06	-65.59	-65.53
19000000.00	19.00	-0.07	-65.70	-65.63
20900000.00	20.90	-0.07	-65.73	-65.66
22800000.00	22.80	-0.07	-65.87	-65.80
24700000.00	24.70	-0.06	-66.01	-65.95
26500000.00	26.50	-0.08	-66.09	-66.01
28400000.00	28.40	-0.08	-66.25	-66.18

Figure 29. File with ".xlsx" extension.

Source: own elaboration.

4.4. Conclusions

This chapter has introduced the measurement method and the measurement principle that has been followed to perform all the measurements. In addition, the equipment with its different characteristics and the measurement setup used in this project have been presented.

Finally, it has been briefly explained how the data processing has been developed to make the results representation and its interpretation.

CHAPTER V: LABVIEW DRIVER

5.1. LabVIEW software

As mentioned before, although the measurements were carried out with the VNA E5071B, the preliminary measurements of the materials were made with the 8753ES. This equipment has a lower dynamic range and bandwidth than the E5071B because it is an older model.

This model also differs in that the communication with the data acquisition equipment, in this case, a computer, must be done by GPIB communication (Fig. 30). For this reason, for this project, it is decided to use a LabVIEW driver to communicate with the equipment.

LabVIEW (Laboratory Virtual Instrument Engineering Workbench) is a platform and development environment for designing systems, with a graphical visual programming language designed for hardware systems and test, control, and design software, simulated or real and embedded.

Figure 30. GPIB IEEE-488 Connector.

Source: own elaboration.

This driver is proprietary to Agilent and is valid for the entire 87XX series. To adapt this driver to the frequency and data treatment and representation characteristics of the project, the interface and some of the features have been re-designed to make it more intuitive for the user and add specific functionalities.

Since this driver will also provide to a company (AIMPLAS) as a tool for data acquisition

with this equipment, certain specifications are set, which have to be modified from Agilent's baseline project.

- Fixed frequency range. It is requested that the user could not enter just any frequency, just only a frequency that was within the bandwidth of the equipment and that could be chosen in X steps.
- Saving of data in a file with ".xlsx" extension through an automatically 'save' button.
- User-intuitive graphical representation of data.
- Annotations on the screen to guide the user, leaving as little slack as possible in the interaction with the interface to avoid errors in the program and the data acquisition process.
- Error-out window to identify an error in the event of such a situation.
- Fixed basic configuration. The data acquisition shall be done in logarithm-magnitude, with a fixed number of segments of 10 and 201 points per segment. This configuration can be changed between specific values as well as the frequency, but there is a note for the user recommending to leave these values by default. These values have been chosen specifically because it has been concluded from various tests that these values give the best time-resolution response.

5.2. GPIB and VISA session

VISA is a standard I/O language for instrumentation programming. VISA by itself does not provide instrumentation programming capability. VISA is a high-level API that calls into lower-level drivers. The hierarchy of NI-VISA is shown in the Fig. 31.

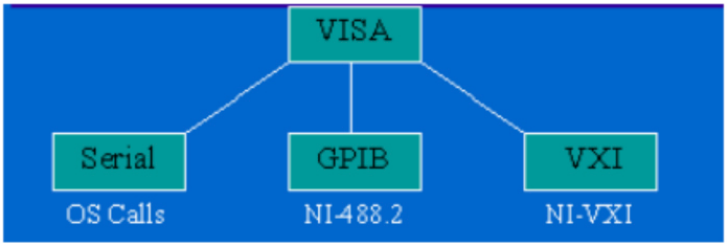

Figure 31. Hierarchy of NI-VISA.

Source: Tutorial visa labview.pdf. (n.d). Google.com.

VISA is capable of controlling VXI, GPIB, or Serial instruments and makes the appropriate driver calls depending on the type of instrument being used. When debugging VISA problems, it is important to keep in mind that this hierarchy exists. An apparent VISA problem could in reality be the results of a bug or installation problem with one of the drivers into which VISA is calling.

One of VISA's advantages is that it uses many of the same operations to communicate with instruments regardless of the interface type. For example, the VISA command to write an ASCII string to a message-based instrument is the same whether the instrument is Serial, GPIB, or VXI. Thus, VISA provides interface independence. This can make it easy to switch interfaces and also gives users who must program instruments for different interfaces a single language they can learn.

The Default Resource Manager is at the highest level of VISA operations. Communication must be established with the Resource Manager at the beginning of any VISA program. This immediately brings up two terms that need to be defined: resource and session.

- **Resource**: An instrument or controller.
- **Session**: A connection, or link, to the VISA Default Resource Manager or a resource.

The reason the VISA Default Resource Manager is so important is because one of its operations is to open sessions to other resources. Sessions must be opened to the instruments the application will communicate with. Therefore, communication with the Default Resource Manager must be established first within an application.

A typical VISA application in LabVIEW would go through the following steps:

1. Open a Session to a VISA Resource.
2. Configure communication on the given resource (configure baud rates, termination character, etc).
3. Perform writes and reads to the instrument.
4. Log out from the resource.
5. Handle any errors that may have occurred.

The LabVIEW application illustrated on the Fig. 32, shows an example of a VISA

session where a session is opened to a GPIB instrument, performs an *IDN? write and reads the specified number of bytes from the device.

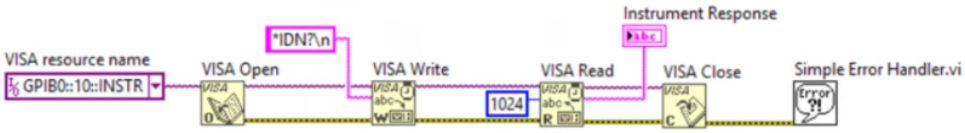

Figure 32. LabVIEW example of VISA session.

Source: own elaboration.

5.3. Project structure in LabVIEW

As mentioned above, LabVIEW is a graphical programming tool, which means that programs are not written in programming code, but are developed graphically through blocks and interconnections, helping their implementation.

As a large number of blocks are already pre-designed, the user can easily create the project, as well as design the graphical interaction interface. This fact allows users to design the interface based on the characteristics and needs of each project. Each LabVIEW project consists of two parts: the front panel and the block diagram.

5.3.1. Front panel

The Front Panel is the interface with the user, it is used to interact with the user when the program is running. The users will be able to observe the data updated in real-time (as the data is flowing, an example would be a calculator, where you put the inputs, and it gives you the result in the output). In this interface, controls (inputs, buttons, or markers) and indicators (outputs or graphs) are defined.

In the Front Panel, it will find all types of controls or indicators, where each of these elements has a terminal assigned in the block diagram, i.e., the user can design a project in the front panel with controls and indicators, where these elements will be the inputs and outputs that will interact with the VI terminal. In the block diagram, all the values of the controls and indicators flow between them when a VI program is being executed.

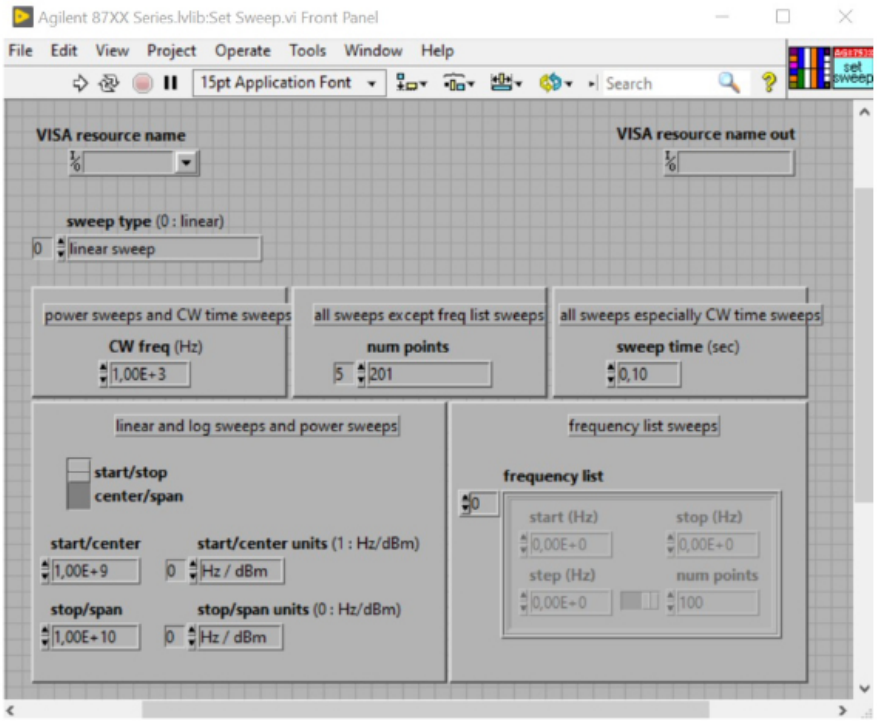

Figure 33. SubVI Sweep Setup Front Panel.

Source: own elaboration.

5.3.2. Block diagram

The Block Diagram is the program itself, where its functionalities and interconnections are defined. Here the icons that perform a concrete function are placed and interconnected with each other. An example of the Sweep Setup SubVI Block Diagram is shown in Fig. 34:

The Block Diagram is the part of a VI that contains the graphical source code known as G. Front Panel controls and indicators appear on the Block Diagram as control terminals. The control terminals for the Front Panel controls are the input where the Front Panel indicators are the output.

Wires connect the terminals to other Nodes and each other to flow the data between them similar to a flow chart. Operational order is dictated by Dataflow. Parts that are not connected are automatically parallelized by the compiler to take advantage of parallel processing that is available in modern multi-core computers.

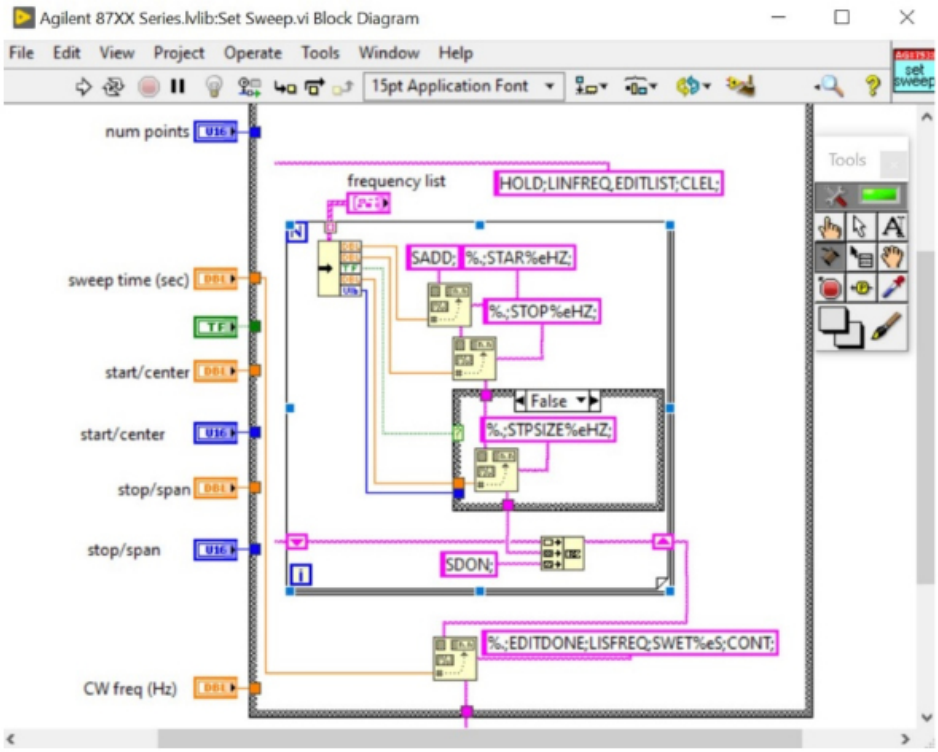

Figure 34. SubVI Sweep Setup Block Diagram.

Source: own elaboration.

In conclusion, LabVIEW is a graphical programming system for applications involving data acquisition, control, analysis, and presentation. The advantages of using LabVIEW can be summarized as follows:

- It provides great flexibility to the system, allowing changes and updates to both hardware and software.
- It allows users to create complete and complex solutions.
- A single development system integrates data acquisition, analysis, and presentation functions.
- The system is equipped with a graphical compiler to achieve the highest possible execution speed.
- It has the possibility of incorporating applications written in other languages.

5.4. Final appearance and results

Afterward, the Front Panel of the re-designed program is shown in Fig. 36. First, you can see a red message indicating the user to select the GPIB port for communication with the VNA 8753ES before executing the program.

If you continue looking from top to bottom, you can see the “port selection” control. This control is where the port number of the connected VNA, once it has been detected by the PC, is displayed. To the right side, the VISA session exit indicator appears to check that the session ends with the correct GPIB port selected.

In the configuration part of the frequency sweep, there are three different fields: number of segments, number of points per segment, and display format.

The control of the “number of segments” is of the “Ring&Enum” type. This type of control has been chosen because it allows setting concrete values to select. In this way, the specification set at the beginning of not allowing the user to select any random value is satisfied. This control allows choosing values between 5 and 30 (in steps of 5).

The same happens with the control of "points per segment". You can choose values between 100 and 500 in steps of 100.

The “display format” control is based on the same type as the two previous ones, but with a slight difference. Instead of numeric values, you can choose between the different types of representation allowed by the VNA (Fig. 35).

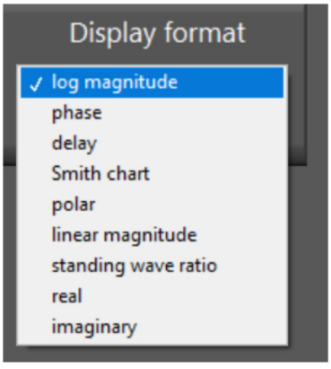

Figure 35. Display format control.

Source: own elaboration.

Below the sweep configuration area, a message appears where it says: "You can leave this configuration by default". In this way, the user is informed that the "default values" are the values with which the measurements have been verified to obtain optimal results.

At the bottom of the interface, there is an "Error handler" where the error message is displayed in case the program fails at any point. In this way, the user can easily identify the problem.

On the right side of the screen, it can be seen the most prominent element, the display. The display indicator has been configured to show attenuation in decibels and frequency in Hz.

The horizontal axis has been kept in Hz due to the limitations of the display indicator, but on the other hand, the numbers are shown with an M for MHz, and a G for GHz. Thus, the user can see the frequency in a very intuitive way.

Finally, there is the great improvement that has been integrated to the driver, the "SAVE" button. With this button, you can export the data directly to an Excel ".tmp" file. The data processing is the same as in section 4.3 described before.

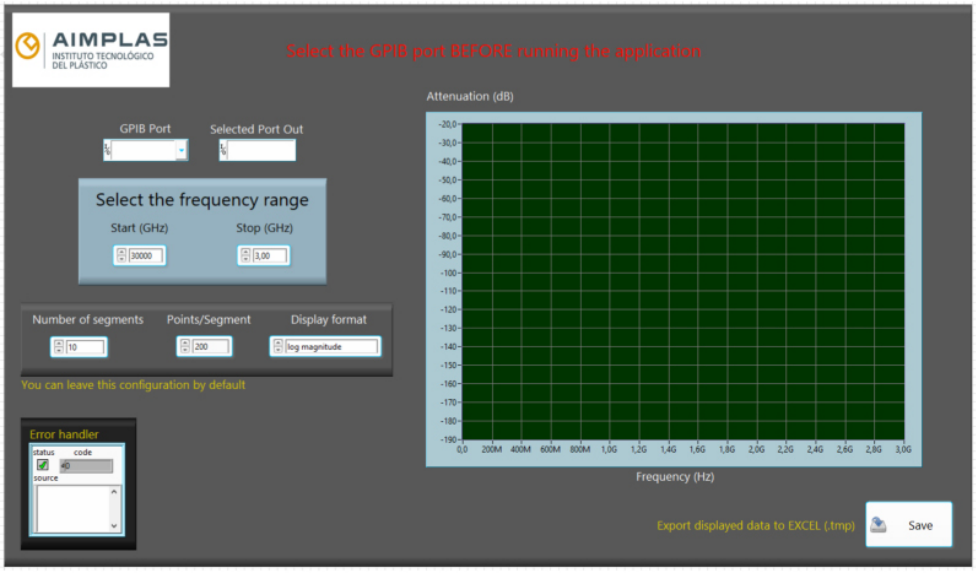

Figure 36. Final appearance of the Front panel.

Source: own elaboration.

On the other hand, the Block Diagram shows the modification of generating the Excel file automatically when the save button is pressed. In addition, at the beginning of the program, the value of the "SAVE" button, the display values, and the VISA session error are reset.

For this purpose, a "Case Structure" of Boolean type has been used, to which the Boolean control of the "SAVE" button is connected. When the value of the control is true, the action of the "True" section is carried out (export data to Excel). Otherwise, nothing is done.

The opening and closing of the VISA session is executed inside the different SubVIs that appear in the main panel of the Block Diagram (Fig. 38).

The program has also been modified to set the frequency in GHz instead of Hz to make it more intuitive to the user, as it can be seen in the upper left side of the Fig. 36.

Another element that stands out, is that at the beginning of the program, it has been added a message. The user must close this message to start the program. The message indicates: "First of all, select the GPIB port".

In this way, the user's attention is called so that it does not run the program without select the GPIB resource port of the VNA, avoiding an error in the program when opening the VISA session (Fig. 37).

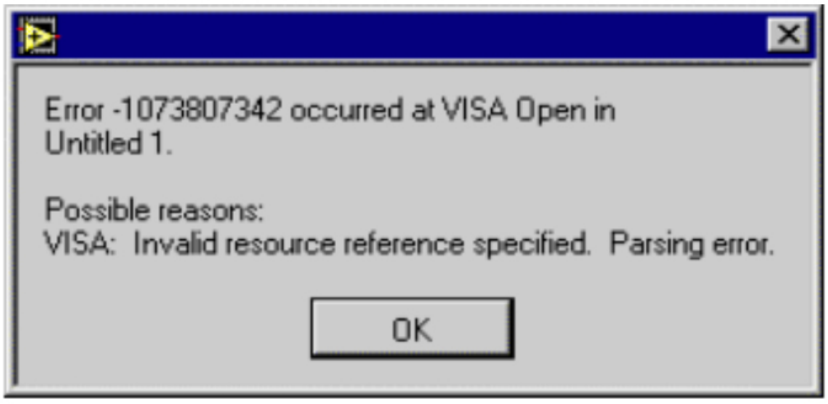

Figure 37. Pop-up dialogue box if an error occurs.

Source: own elaboration.

For this purpose, a "flat sequence" has been used. This structure allows to pause the execution of the program at a certain point and not continue until the action enclosed in the first sequence is finished. The execution order is from left to right.

It is also important to mention that the appearance of the program has been modified by adding colors to the different levels, basically to make it more visual and intuitive for the user. It has also been compacted so that it takes up as minimal space as possible.

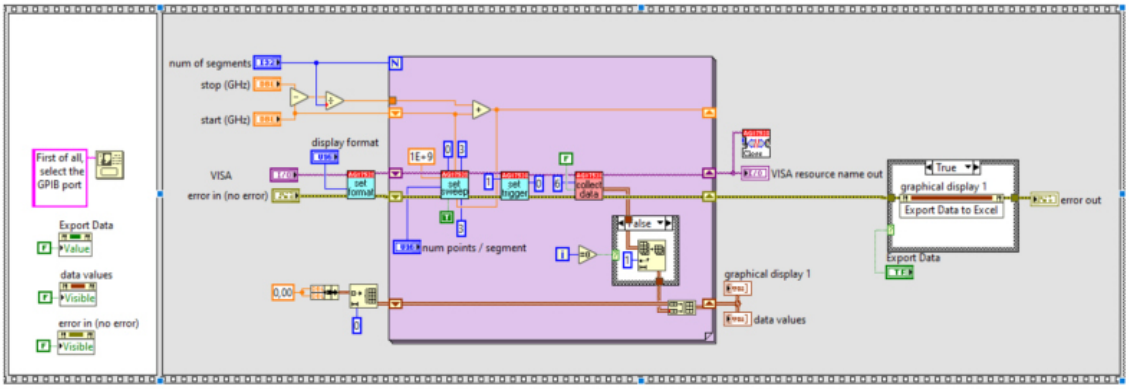

Figure 38. Final appearance of the Block diagram.

Source: own elaboration.

5.5. Conclusions

This chapter has dealt with the development of the specific LabVIEW driver for the 8753ES, satisfying the objectives fixed in subsection 1.2. Adaptation of the software for analyzing the EM properties of materials in the 5G frequency range.

In addition, the main aspects of a VISA session, which are the key aspects for GPIB communication with the equipment, have been explained.

Once the chapter has been concluded, it can be said that the specifications required by AIMPLAS in terms of software operation and interface have been fulfilled.

CHAPTER VI: RESULTS AND DISCUSSION

6.1. Introduction

In this section it will be shown the different measurements performed of the obtained specimens. An alternative measurement method will also be presented and the differences with the standard method.

First of all, it will be discussed the first measurements carried out as a test with some samples of the same material with a different concentration of CNT.

Then, the main measurements of the research will be presented, showing the response of the eight different samples obtained in the manufacturing process.

Finally, as already mentioned, an alternative measurement method is proposed and the results obtained will be evaluated.

It is important to remark that, at this point, there are going to observe measurements in two different frequency ranges: FR1 (sub-6 GHz) and the ASTM 4935-18 standard frequency range (from 30 MHz to 1.5 GHz).

In each section, the specific frequency range of the different measurements is indicated.

6.2. Shielding effectiveness as a function of CNT concentration

Three samples with different CNT compositions have been measured. These three samples are composed of the same material but present three different CNT concentration: 5%, 7%, and 10%. In this section, the SE will be measured as a function of the percentage of carbon nanotubes to see how it influences shielding effectiveness.

The test samples are shown in Fig. 39. It clearly illustrates the three pieces that form the reference sample (the washer and the disk-shaped sample) and the load, following ASTM 4935-18 standard.

As mentioned before, all samples must have the same thickness (approximately 2.3 mm) since this is an influential factor in the measurement of shielding effectiveness. In this way, the influence of sample thickness is eliminated, and the three

measurements can be compared with each other.

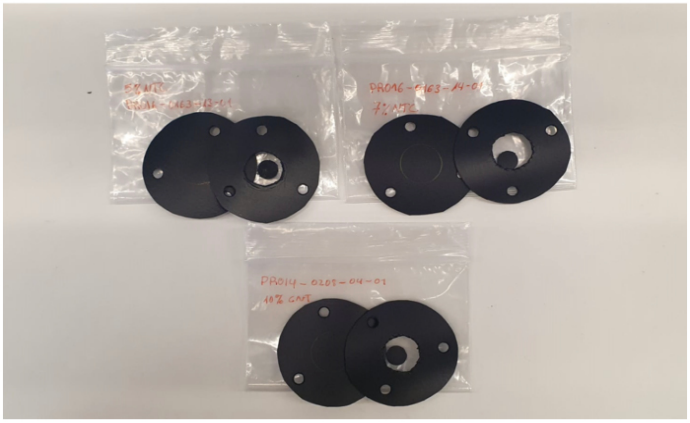

Figure 39. Test samples of different percentage of CNT.

Source: own elaboration.

6.2.1. Testing the influence of the sample position

As explained above, the samples are composed of CNT. Due to the tubular shape of the CNTs, depending on the manufacturing process, they can present random positions and directions. This fact implies that the samples are not homogeneous and, theoretically, the SE could be affected by the position of the test sample in the probe.

This is why it has been decided to perform control measurements by rotating the sample in 120º angles as shown in Fig. 40. In this way, the SE is obtained in the three possible positions of the sample to see how the direction of the CNTs affects the response of the shielding effectiveness.

Figure 40. Rotation of the 10% CNT sample in different angles.

Source: own elaboration.

The Fig. 41 shows the measured SE of the sample with 10% CNT composition. This is the most critical specimen because it has the highest percentage of CNT of the available samples.

The black trace corresponds to the first SE measurement. On the other hand, the grey trace corresponds to the SE measurement by turning the sample 120º to the left (position two). Finally, the red one represents the third position, with a further 120º turn (240º overall) to the left.

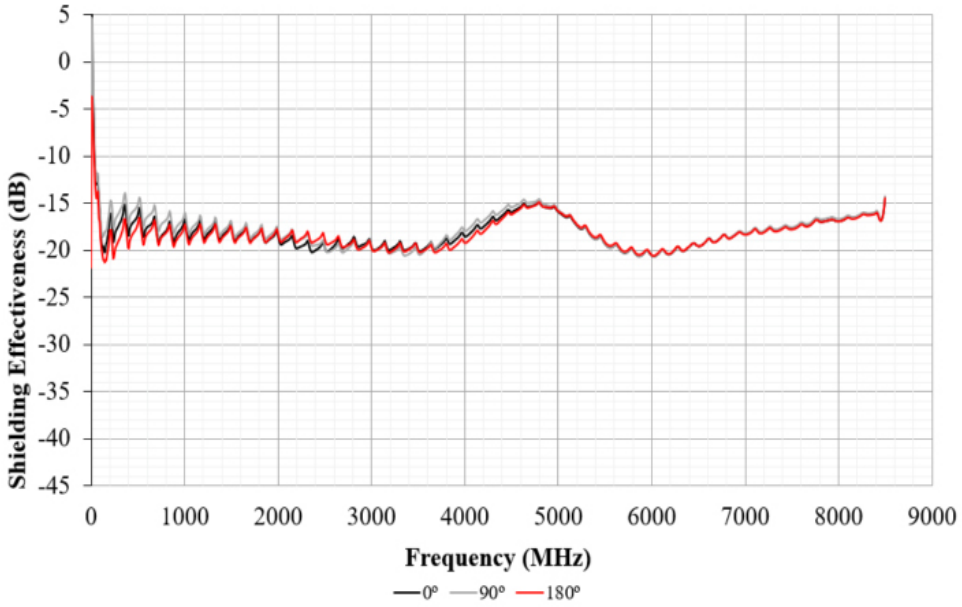

Figure 41. Shielding effectiveness of the 10% CNT composite depending on the position of the test sample.

Source: own elaboration.

The graph shows that the traces are sufficiently similar to each other, so it can be said that the influence of the CNT position can be disregarded. The biggest difference between the three traces can be seen at low frequencies, but this is not relevant in this project since the frequencies of interest are above 30 MHz.

6.2.2. Comparing the SE of different CNT concentrations

Once the influence of position could be disregarded, the samples with different concentrations were measure.

For this purpose, a 'SMOOTH' of 1.5% and 1201 points were configured in the VNA. The measured frequency range corresponds to the maximum bandwidth of the equipment.

It should be considered that although it is possible to get an idea of the behavior of these materials over the whole frequency range, the probe follows the ASTM 4935-10 standard so that frequencies above 1500 MHz would not be considered.

Real permittivity of polymer nanocomposites is a measure of the number of micro-capacitors and the polarization centres. Polarization centres originate from the defects in the nanofiller structure, while the micro-capacitors are simply formed by nanofiller particles/aggregates acting as electrodes filled with insulating polymeric material. Thus, the increase in CNT loading increases e0 because of the increase in the number of these micro-capacitors and structural defects.

So, the increase in conductivity is strongly dependent on nature, concentration and aspect ratio of filler particles as well as type and morphology of host ICP matrix [41].

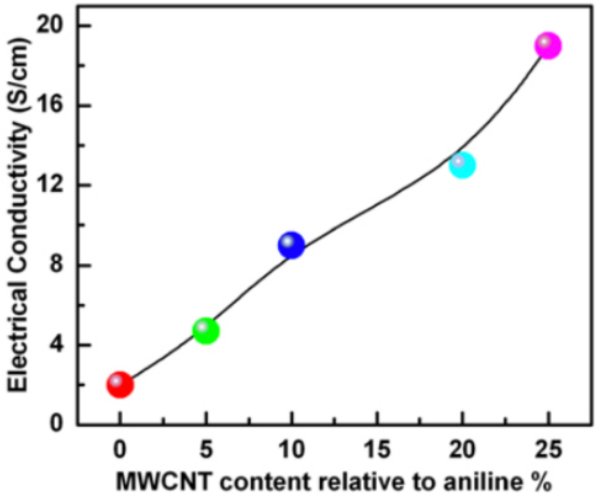

Figure 42. Dependence of electrical conductivity of MWCNT nanocomposites on MWCNT content.

Source: [41].

The Fig. 43 shows the shielding effectiveness of samples with different CNT compositions: 5%, 7%, and 10%. Theoretically, as the percentage of carbon nanotubes

increases, the SE should increase as well. This effect can be seen between the 5% (red trace) and 7% (black trace) responses. However, this is not applicable for the sample with the 10% CNT composition, since the SE does not increase compared to the 7% sample.

This fact may be due to the composition of the samples because, as discussed above, they are not homogeneous samples with a uniform dispersion of CNTs that follow a linear trend concerning the SE.

Relatively uniform dispersion of CNTs can be achieved in polar polymers such as nylon, polyaniline and polyamide because of the strong interaction between the polar moiety of polymer chains and the surface of the CNTs.

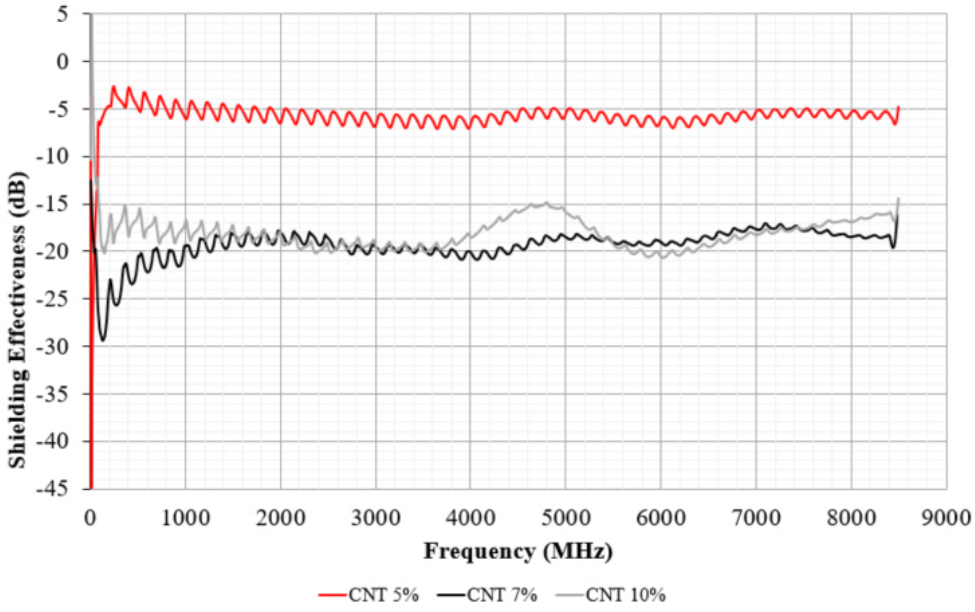

Figure 43. Shielding effectiveness as function of CNT content.

Source: own elaboration.

6.3. Measurement of the composite samples

This section is focused on showing the results corresponding to the measurement of eight sample composites under test. A comparison between the carbon fiber and glass fiber's SE performance is carried out by combining them with the three conductive materials.

6.3.1. ASTM 4935-18 frequency range (30 MHz to 1.5 GHz)

Firstly, the different materials' shielding effectiveness is evaluated by considering the frequency range defined in the ASTM 4935-18 standard (30 MHz to 1.5 GHz). Fig. 44 shows the shielding effectiveness provided by the composite laminates samples based on CF reinforcement (solid traces) and GL reinforcement (dashed traces).

It can be observed that the GF samples without any conductive material do not provide attenuation, whereas the CF sample can provide significant SE. The CF sample provides an attenuation between around -55 dB to -75 dB, considering the frequency range from 100 MHz to 1.5 GHz.

When a conductive material is added to the CF reinforcement, a similar SE is obtained. The addition of the MW-CNT conductive material results in improving the SE response by about 3 dB. Specifically, if the 1 GHz frequency point is considered, the CF+MW-CNT sample shows an attenuation of-73.6 dB, whereas the CF sample of -70.3 dB. Regarding the CF+Gr-Ni and CF+Cu samples, the original CF material is able to provide a better response. If these two combinations are compared, the CF+Gr-Ni is able to show higher SE values than CF+Gr-Ni from 550 MHz.

Nevertheless, the influence of the conductive materials analyzed for the CF sample is not correlated in the case of being combined with GF. Thereby, the GF+Cu is the GF based combination that represents the best performance.

However, the opposite of what happens with CF, GF's combination with the conductive material based on MW-CNT provides the worst response in terms of shielding effectiveness. The GF+Gr-Ni sample provides a similar response to GF+Cu up to 450 MHz, but its effectiveness is reduced from that frequency point.

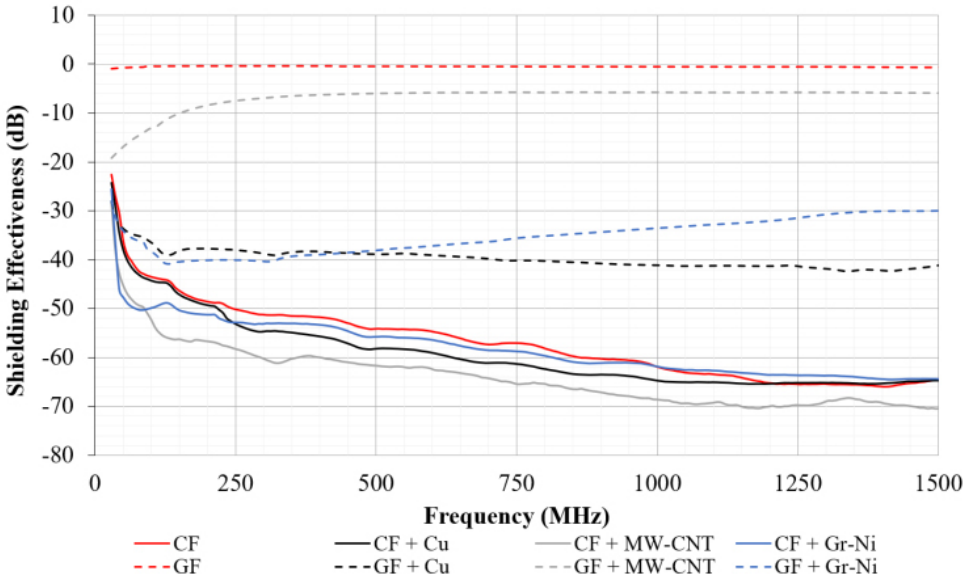

Figure 44. Shielding effectiveness in the ASTM4935-10 bandwidth.

Source: own elaboration.

6.3.2. Sub-6 GHz Frequency range (410 MHz to 7125 MHz)

Whereas the frequency range established by the ASTM 4935-18 standard is limited to frequencies below 1.5 GHz, measures have been carried out from 300 kHz to 8.5 GHz, to observe the tendency of the behavior of the different materials in the FR1 frequency range (410 MHz – 7125 MHz) [22].

Fig. 45 shows the measurement of reference specimens of the different materials. These measurements provide an approximate representation of the behavior of these materials in a higher frequency range. It can be seen that the method provides flat responses, although it can be noted that there is an uncertainty range between 4 GHz and 5 GHz, which has not been considered large enough to discard measurements made at these frequencies.

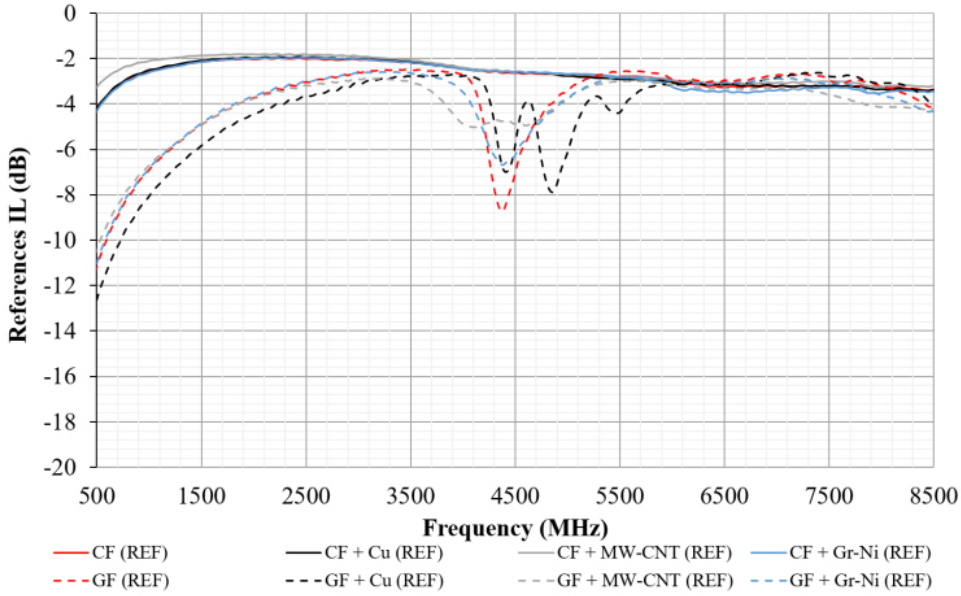

Figure 45. Insertion loss of the reference specimens.

Source: own elaboration.

As mentioned before, although the range defined in the standard is between 30 MHz and 1.5 GHz, measurements have been carried out in the frequency range from 300 kHz to 8.5 GHz. This is because the aim of the study is to observe the behavior at higher frequencies and get an approach of the SE value in frequencies above 1.5 GHz.

In contrast with the results presented in Fig. 44, Fig. 46 shows the shielding effectiveness provided by the same composite laminates samples, but considering the sub-6 GHz bandwidth (410 MHz – 7125 MHz). It is observed that the trend of the SE response is maintained, so it is possible to obtain an approximation of the performance of the materials at higher frequencies.

By extending the frequency range beyond that described in the ASTM 4935-18 standard, it can be observed how certain parasite resonances become evident, particularly in the traces of the GF+Cu combination specimen, reaching values of approximately-10 dB at frequencies around 4.2 GHz.

Note also an uncertainty bandwidth between 3.1 GHz and 4.0 GHz in the responses of the CF samples, where the resonance of the GF+Cu composite, reaches a value of

-42 dB. This means that the most significant variations in the responses are found in those materials whose conductive material is copper.

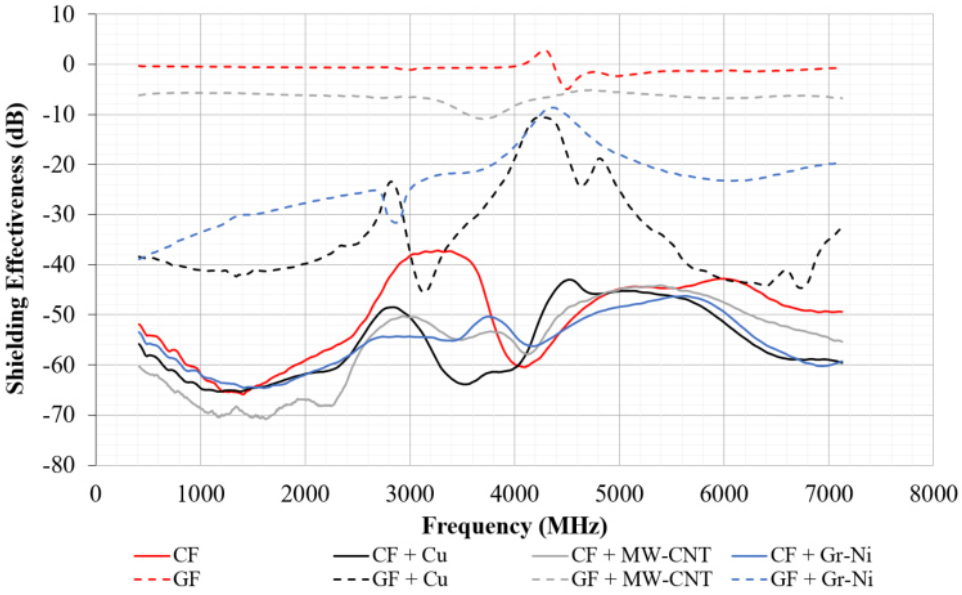

Figure 46. Shielding effectiveness of the composite materials.

Source: own elaboration.

At this point, there are some generic findings obtained from the results. For example, for the GF composites, it has been seen that without any conductive material, does not provide any attenuation and, it can also be said that the best response is given by the GF+Cu combination. In contrast, the CNT combination, in this case, is the one that gives the worst attenuation.

On the other side the Gr-Ni combination that gives a response quite similar to the copper and does not introduce any improvement over the other combinations.

Concerning the CF-based composites, the sample without any conductive material shows considerable attenuation. Regardless of the conductive material added to the CF, the responses are very similar between them, being the best the one with CNT contrary to what happens with GF.

And the last thing is that the original CF sample has a higher attenuation than the combinations with GR-Ni or copper in the standard frequency range shows all the

aspects mentioned above:

Table 3. Conclusions drawn from the measurements.

Glass Fiber Composites	Carbon Fiber Composites
GF samples without any conductive material does not provide attenuation	CF sample provides attenuation around-55 dB to-75 dB
GF+Cu is the GF-based combination that represents best performance	CF + conductive material provides similar SE response
MW-CNT provides the worst SE response	MW-CNT conductive material results in improving the SE response in 3dB @ 1 GHz
GF+Gr-Ni provides similar response to GF+Cu up to 450 MHz	Original CF samples provides higher SE values than CF+Gr-Ni and CF+Cu composites
-	CF+Gr-Ni results in higher SE values than CF+Cu from 550 MHz

Source: own elaboration.

6.3.3. Shielding effectiveness of the copper mesh

Copper mesh conductive material has been evaluated in terms of SE by obtaining the reference and load transmission parameters. This material can provide a significant SE performance and can be considered as a reference in order to determine composite laminates performance evaluated in this contribution. Fig. 47 shows the SE for this conductive material as a reference measurement.

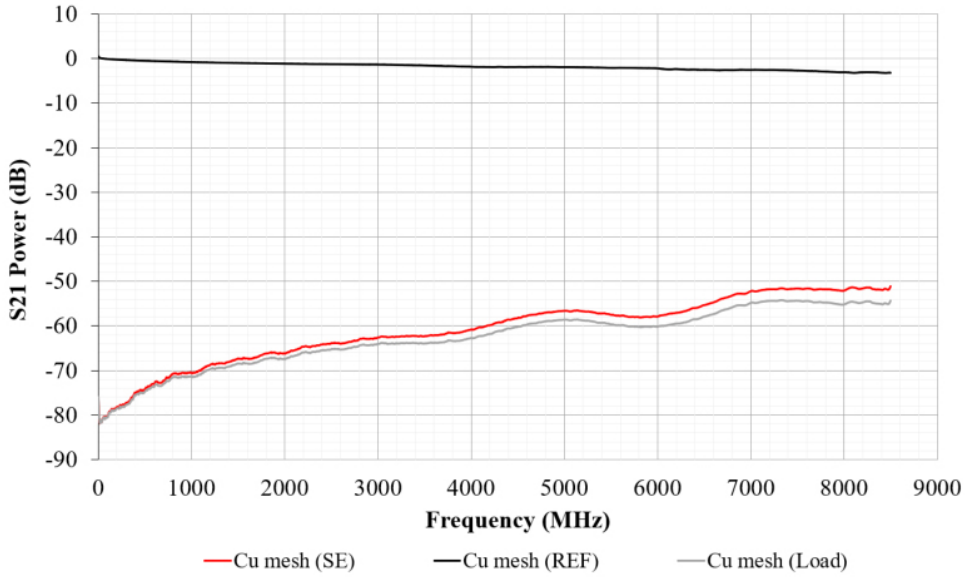

Figure 47. Copper mesh shielding effectiveness.

Source: own elaboration.

As it is clearly in the image, the IL of the reference sample (black trace) provides a nearly flat response up to about 3.5 GHz. This is why the load (gray trace) and the SE (red trace) are almost coincident up to that frequency.

It is important to note that both, the IL measurement of the load and that of the reference, are not absolute values like the SE but are values taken directly from the VNA.

6.4. Comparing the SE results with signal generator method in function of the power injected

6.4.1. Introduction to the method

First of all, it is worth mentioning that the aim of proposing an alternative measurement method is to check whether the proposed setup provides a higher dynamic range than the VNA method. In this case, dynamic range is defined as the margin between the reference level and the background noise of a given system, measured in decibels. This aspect is one of the main problems when talking about the characterization of shielding materials since the objective is that the attenuation of these materials is as high as possible.

According to the ASTM-4935 standard document, the dynamic range of the equipment can be checked by comparing the maximum signal level obtained with a reference specimen to the minimum signal level obtained when using a metallic specimen, like aluminum foil (Fig. 48) [42].

Figure 48. Aluminium sample.

Source: own elaboration.

Fig. 49 shows an example of the measurement of the dynamic range corresponding to the VNA E5071B in the standard frequency range. As it can be seen, the load specimen of the metallic sample, provides an SE around -90 dB, which corresponds to the data shown in the equipment datasheet.

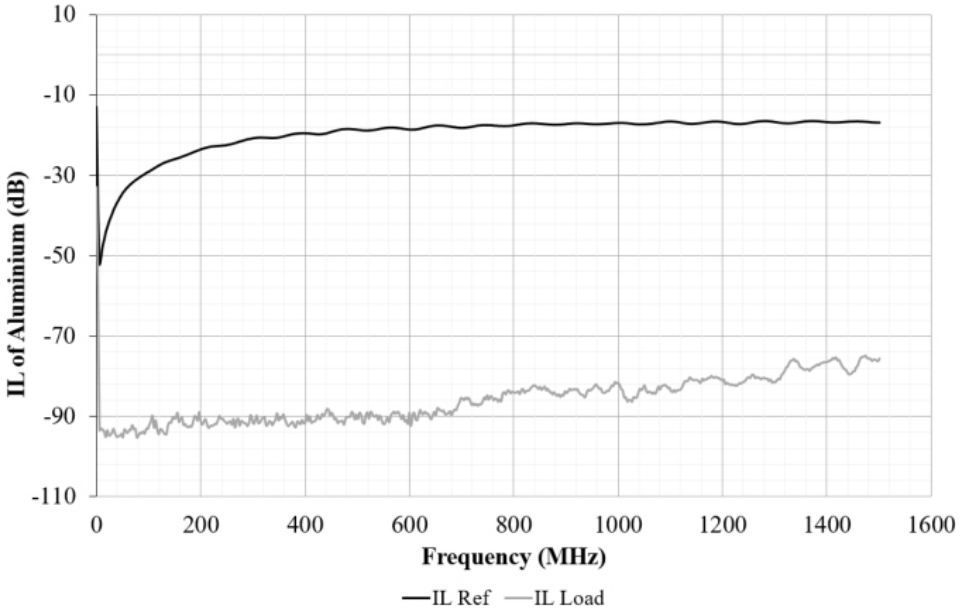

Figure 49. Measurement of the dynamic range of the VNA E5071B.

Source: own elaboration.

Increasing the effective dynamic range in the measurement is theoretically possible because using two different types of equipment, a spectrum analyzer (SA) and a signal generator, it is possible to configure two different signals with two different stages to measure the load and reference samples. In addition, the SA has an input stage with a preamplifier and several attenuators that increase the versatility of the equipment configuration to perform a measurement.

6.4.2. Measurement procedure

The procedure that is going to be used to measure the different samples with this method is based on generating a frequency sweep (10 MHz – 3 GHz) of sinusoidal signals of different powers and acquiring them with a spectrum analyzer for their representation.

This method requires two different devices: a spectrum analyzer and a signal generator. The signal generator must be a source capable of generating a sinusoidal signal over the desired portion of frequency range specified in the ASTM 4935-18 standard. It is also needed a 50 Ω output port to minimize reflections due to

mismatches.

A good frequency sweep configuration is needed in order to increase the effective dynamic range for SE measurements. In particular, the Agilent N5171B EXG Analog Signal Generator (Fig. 50) will be used as sinusoidal signal generator. This equipment is limiting in terms of the frequency range, since its bandwidth extends from 9 kHz to 3 GHz.

Figure 50. Keysight (Agilent) N5171B EXG Analog Signal Generator.

Source: own elaboration.

The main fields of the sweep configuration are described below. A linear sweep has been selected. In addition, the start frequency is set to 10 MHz, since frequencies in the order of kHz are not to be considered. The maximum frequency corresponds to the maximum frequency of the equipment, 3 GHz. The number of points chosen for this method was 1600.

As mentioned above, different powers will be tested. This is the reason why the "Amplitude Start (dBm)" field will be modified according to the desired power.

On the other hand, the SA is used in the same way as the VNA E5071B to measure the S21 parameter of the sample introduced in the specimen holder. Specifically, the equipment to be used is the Keysight N9010A.

The common configuration of the SA (Fig. 51), regardless of the measured specimen is: Resolution BW (RES BW) of 8 MHz and Video Bandwidth (VBW) of 50 MHZ.

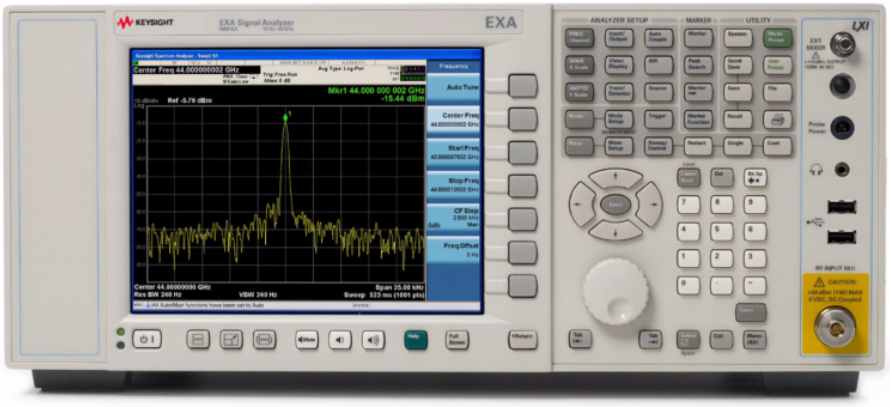

Figure 51. Spectrum analyzer Keysight N9010A.

Source: own elaboration.

The complete experimental setup used to perform the measurements using the signal generator method is shown in Fig. 52:

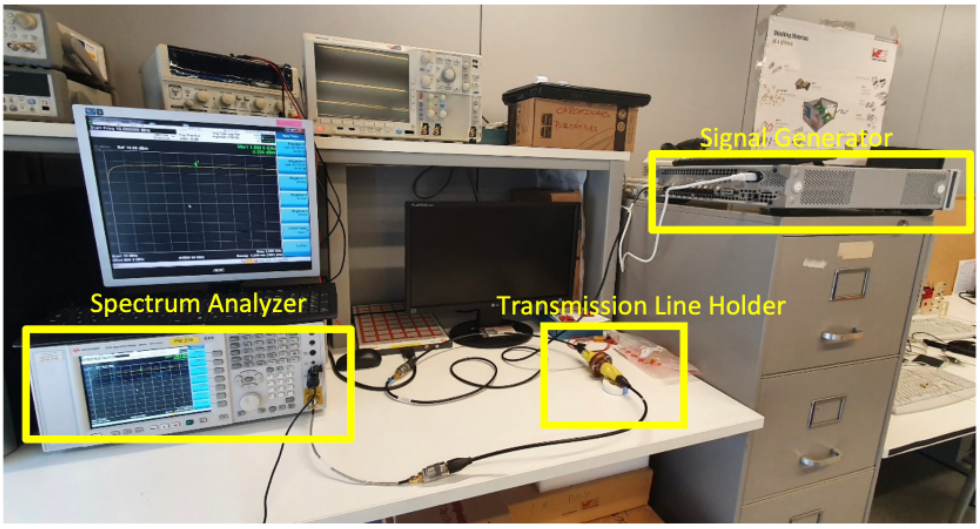

Figure 52. Signal generator setup method to measure SE of the 5% CNT sample.

Source: own elaboration.

Since a different output power of the signal generator has to be set depending on whether the reference sample or the load is being measured, it was decided to perform a test with three different powers:-10 dBm, 0 dBm, and +10 dBm.

To capture the trace resulting from the frequency sweep, the SA presents different options: “Clear White”, “Trace Average”, “Max Hold” y “Min Hold”.

Finally, it has been decided to use the "Max Hold" option for data capture. With enabled max hold function, the displayed trace shows the maximum values that the analyzer acquired since the start of the measurement [43]. The capture mode menu with the "Max Hold" option selected is displayed in the Fig. 53:

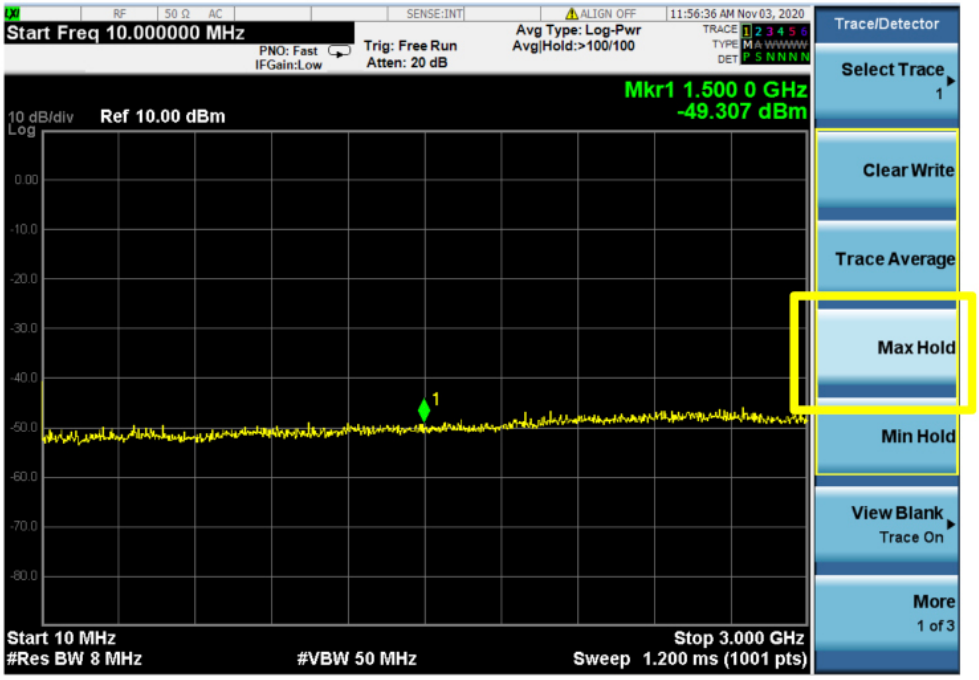

Figure 53. Open circuit response with the “Max hold” option selected.

Source: own elaboration.

The objective of these measurements is to observe if the effect of the power influences the measurement, or if on the opposite, when subtracting the insertion losses of the load and the reference, the effect is canceled and the same measurements are obtained as with the VNA method.

The IL responses of the reference (Fig. 54) and load (Fig. 55) specimens are shown in the figures below:

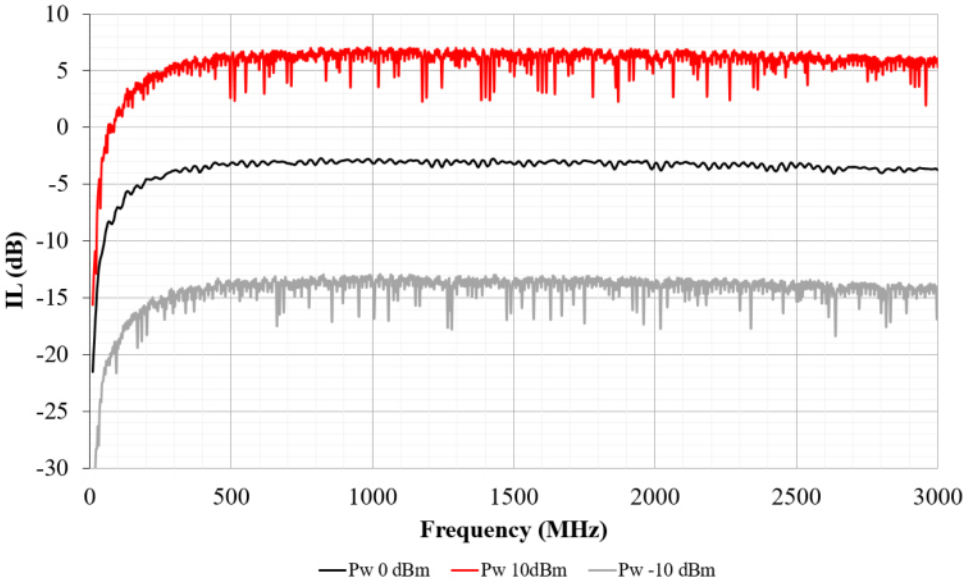

Figure 54. Insertion Loss in dB of the 5% CNT reference specimens in function of the power injected.

Source: own elaboration.

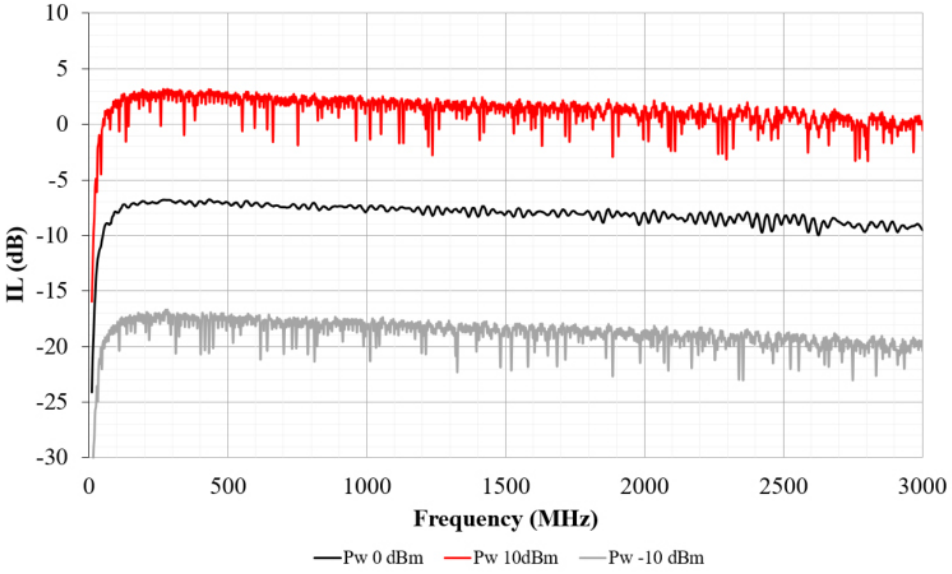

Figure 55. Insertion Loss of the 5% CNT sample Load specimen in function of the power injected.

Source: own elaboration.

In this case, the IL measurements are not absolute values, and as can be seen in the images above, they are dependent on the power injected with the signal generator.

Once some measurements had been made to verify the effectiveness of the method, the results were compared with the ASTM 4935-18 standard method.

The Fig. 56, shows the three different responses of the 5% CNT sample in terms of the power injected. It can be seen that, although the traces are noisy, it can be seen how the trend is coincident for all the three traces, so the preliminary thought that the power cancels out is confirmed.

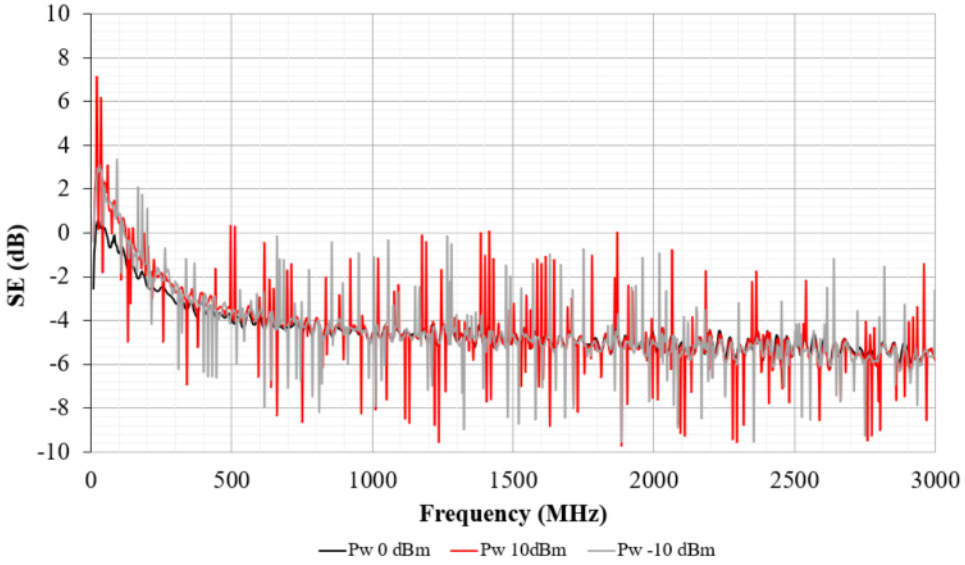

Figure 56. Shielding effectiveness of the 5% CNT sample in function of the power injected.

Source: own elaboration.

On the other hand, Fig. 57 shows the comparison between the three previous traces and the response obtained using the VNA E5071B (yellow trace).

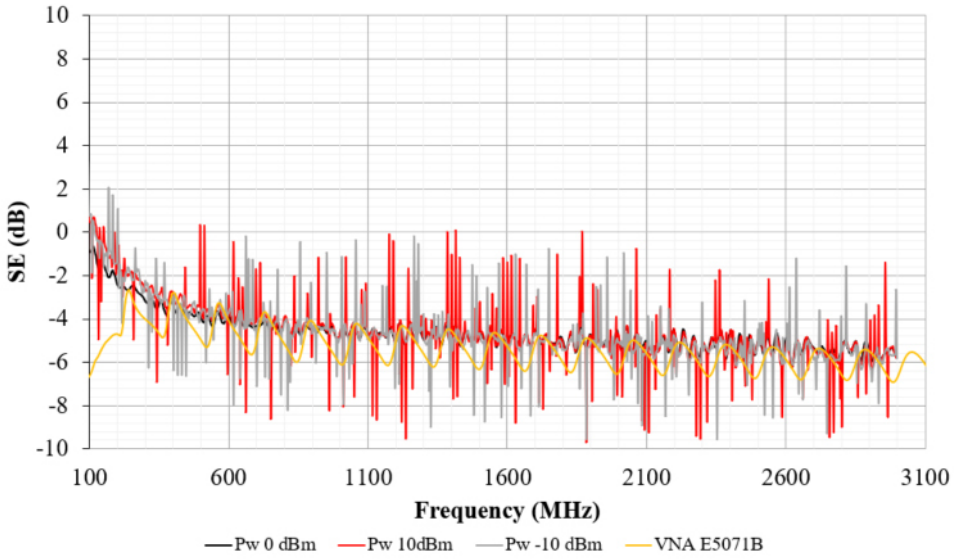

Figure 57. Comparing the SE with the E5071B method.

Source: own elaboration.

In this case, since it is the subtraction of the IL measurements of the reference and load samples represented above, the SE measurement is an absolute measure.

Since it has been verified that the injected power does not affect the measurements, it has been searched for the most effective configuration in order to maximize the dynamic range of the equipment.

For this purpose, as mentioned above, depending on whether the sample is the reference or the load, the equipment is configured in two different ways. These configurations are shown in:

Table 4. Equipment configuration depending on the measured specimen.

	Spectrum Analyzer		**Signal Generator**
	Internal Pre-Amplifier	Internal Attenuator	Power Injected
Load Specimen	YES	0 dB	+ 18 dBm
Reference Specimen	NO	20 dB	- 15 dBm

Source: own elaboration.

Once the measurements have been made, it has been extracted different aspects to consider about this measurement method. Firstly, it should be noted that this method requires two types of equipment to carry out the measurements. Compared to the standard procedure, which requires only one device, this is a disadvantage.

Another aspect to take into consideration is that the frequency sweep has to be configured in the signal generator. Therefore, it is necessary to perform several tests to find the sweep setup that best corresponds to the sample being measured, which implies more preparation before making a measurement.

It is also important to remark that the bandwidth of the method is limited to 3 GHz since it is the maximum frequency of the two available equipment used to perform the measurements.

It should be pointed out that traces are not as clean as with VNA E5071B as it can be seen in the previous Fig. 57.

Something that is certainly a drawback in this method, is that the configuration of the spectrum analyzer and the signal generator has to be changed depending on whether the sample introduced is the reference or the load. This implies changing the setup configuration, which can lead to incorrect parameter selection and measurement errors.

6.5. Conclusions

This section there has been presented the results of three different types of tests. First, samples of the same material were measured as a function of CNT concentration. The influence of the sample position on the probe has been tested, and then the SE has been obtained.

On the other hand, the SE of the eight main samples of this project has been measured in two different frequency ranges, the ASTM 4935-18 standard and the sub-6 GHz. Then, conclusions have been drawn by comparing the carbon fiber samples with the glass fiber samples.

Finally, an alternative measurement method based on a signal generator and a spectrum analyzer has been proposed, to increase the dynamic range of measurement. The results of this method have been presented as a function of the power injected and compared with the results of the standard measurement method.

CHAPTER VII: CONCLUSIONS

7.1. Conclusions

To accomplish, there will be a summary of the conclusion drawn form the results obtained and the different methods used to perform the measurements.

First of all, the conclusions obtained from the measurements of the samples with different CNT concentrations will be presented. Then, the analysis of the results obtained from the measurements of the eight main samples of the project according to the ASTM 4935-18 standard will be analyzed.

Finally, the conclusion drawn from the measurement method of the signal generator will be discussed, comparing this method with the previous one.

7.1.1. CNT percentage samples

In conclusion, it is notable that CNTs-based polymer nanocomposites present an array of possibilities for their use in various technology developments. The electrical properties and dependent applications of CNTs-based nanocomposites, specifically, EMI shielding, are already satisfactory, though the scope for improvement cannot be ruled out. Incorporation of CNTs into a polymer matrix is a very attractive way to combine the mechanical and electrical properties of individual nanotubes with the advantages of plastics.

The results demonstrate that CNTs increase the SE of the EMI composites, but it cannot be said that the increase in shielding effectiveness will be linear. This may be due to the heterogeneity of the material and its internal structure. This is why it can be said that no-conclusive results have been obtained, as can be observed in the samples with 7% and 10% CNT.

To select and design absorbing materials in a specified frequency range, one should take into account not only the CNTs concentration but also the kind of polymer and thickness of materials.

7.1.2 Composite samples

EMI shielding effectiveness in the FR1 frequency range of 5G has been studied. Two types of materials based on carbon fiber and glass fiber have been compared, adding to both three types of conductive materials to give them metallic properties.

It has been observed how the different materials perform in the specified frequency range, giving a preliminary idea of how they might work at higher frequencies for applications requiring EMI shielding against the ever-increasing 5G technologies.

Firstly, it has been concluded that the CF presents a higher attenuation than the GF without introducing any conductive material. Furthermore, it has been observed that combining conductive materials with the CF composite gives very similar results to the original response, regardless of the material introduced. Concerning this, it would be concluded that the combination that provides the best results to CF composites is CF+MW-CNT, while for GF, the best combination is GF+Cu.

It has to be remarked that these types of characterizations are very relevant from a technological and industrial point of view. Specifically, for automotive and related sectors, the use of EMI shielding based on plastic materials has many advantages such as the manufacturing cost reduction.

Considering this, in the automotive sector, particularly the vehicle of the future, the weight of those elements in which specific structural characteristics of rigidity, protection against impact as well as vibration absorption are not required, is a frequent area of work, aimed above all at reducing the consumption of vehicles. This is why developing these types of plastic materials with metallic properties is very important nowadays.

Consequently, the selection of these plastic materials and their conductive composite polymers is not arbitrary, as it has been demonstrated. Some of the samples analyzed and, specifically, those based on CF composites, present a considerable attenuation to be able to replace metallic materials, thus eliminating the disadvantages that these materials entail.

7.1.3. Signal generator method

An alternative method was proposed to perform the measurements according to the ASTM 4935-18 standard. Once the tests and measurements were performed to verify the effectiveness of the method, the results were compared with the values obtained with the VNA E5071B.

When it was observed that the results were similar in terms of magnitude, some conclusions were drawn from them. The most relevant point is that this method involves the use, and therefore the configuration, of two different instruments. In

addition, both configurations have to be modified depending on the sample being measured (reference or load specimens).

On the other hand, the bandwidth is limited to 3 GHz, as opposed to the 8.5 GHz of the VNA. In addition, the traces are noisier than with the VNA.

With all these aspects, it has been concluded that the dynamic range of the equipment is not increased enough. So, the negative aspects of the method do not compensate for the low increase of the dynamic range.

For this reason, it can be said that the most appropriate method for measuring composite plastic materials according to ASTM 4935-18 standard is the method based on the measurement of IL with the VNA, in this case, the VNA E5071B.

7.2. Future lines of development

The following are different aspects that have been considered interesting for future works and research related to the developed study.

The first of the possible lines of development that is interesting to comment, would be the possibility of measuring in the 5G FR2 frequency range. Since these are such high frequencies, it is important to mention that it would be necessary to have new equipment with an extended bandwidth that would allow measuring the different materials at these frequencies.

Another aspect to consider would be to investigate other materials with the ability to replace conventional metallic materials measuring the SE of these materials. In this way, it would be possible to compare the results obtained from the study with other materials and observe their behavior in the entire 5G frequency range.

Other potential improvements that could be included in the project would be concerning the LabVIEW driver. It could be interesting to incorporate functionality that would allow generating a compatible file type with MATLAB software. This is an application widely used in the field of massive data processing and analysis, so this functionality would allow simply using this tool.

Finally, it is interesting to point out that this project is involved in the project "strategic lines of collaboration 2021". This fact implies that the aspects previously mentioned as future lines of development are not only observations but can be carried out.

REFERENCES

[1] Idris, F. M., Hashim, M., Abbas, Z., Ismail, I., Nazlan, R., & Ibrahim, I. R. (2016). Recent developments of smart electromagnetic absorbers based polymer-composites at gigahertz frequencies. *Journal of Magnetism and Magnetic Materials, 405,* 197–208.

[2] Victoria, J., Suarez, A., Martinez, P. A., Alcarria, A., Gerfer, A., & Torres, J. (2020). Improving the efficiency of NFC systems through optimizing the sintered ferrite sheet thickness selection. *IEEE Transactions on Electromagnetic Compatibility, 62*(4), 1504–1514.

[3] Victoria, J., Suarez, A., Torres, J., Martinez, P. A., Alcarria, A., Martos, J., Garcia-Olcina, R., Soret, J., Muetsch, S., & Gerfer, A. (2018). Transmission attenuation power ratio analysis of flexible electromagnetic absorber sheets combined with a metal layer. *Materials, 11*(9). https://doi.org/10.3390/ma11091612

[4] Paul. (2006). *Introduction to electromagnetic compatibility.*

[5] Matsushita, N., Nakamura, T., & Abe, M. (2003). Spin-sprayed Ni–Zn–Co ferrite films with high μr″>100 in extremely wide frequency range 100 MHz–1 GHz. *Journal of Applied Physics, 93*(10), 7133–7135.

[6] Ott. (2011). *Electromagnetic compatibility engineering.* Wiley.

[7] Li, X., Wang, G., Yang, C., Zhao, J., & Zhang, A. (2021). Mechanical and EMI shielding properties of solid and microcellular TPU/nanographite composite membranes. *Polymer Testing, 93*(106891), 106891.

[8] Cheng, H.-C., Chen, C.-R., Hsu, S.-H., & Cheng, K.-B. (2020). Electromagnetic shielding effectiveness and conductivity of PTFE/Ag/MWCNT conductive fabrics using the screen printing method. *Sustainability, 12*(15), 5899.

[9] Seiler, W. (n.d). *EMI shielding for thermoplastic housings*. https://www.fst.com

[10] Naseer, A., Mumtaz, M., Raffi, M., Ahmad, I., Khan, S. D., Shakoor, R. I., & Shahzada, S. (2019). Reinforcement of electromagnetic wave absorption

characteristics in PVDF-PMMA nanocomposite by intercalation of carbon nanofibers. *Electronic Materials Letters, 15*(2), 201–207.

[11] Royal DSM N.V. (n.d.). Dsm.Com. Retrieved September 29, 2021, from https://www.dsm.com

[12] Jadhav, A. (2018). *Autonomous Vehicle Market by Level of Automation (...) Global Opportunity Analysis and Industry Forecast, 2019-2026.* Allied Market Research.

[13] Khan, M. K., & Quadri, A. (2021). Augmenting cybersecurity in autonomous vehicles: Innovative recommendations for aspiring entrepreneurs. *IEEE Consumer Electronics Magazine, 10*(3), 111–116.

[14] Liu, Z., Jiang, H., Tan, H., & Zhao, F. (2020). An overview of the latest progress and core challenge of autonomous vehicle technologies. *MATEC Web of Conferences, 308*, 06002.

[15] Aerts, S., Verloock, L., Van Den Bossche, M., Colombi, D., Martens, L., Tornevik, C., & Joseph, W. (2019). In-situ measurement methodology for the assessment of 5G NR massive MIMO base station exposure at sub-6 GHz frequencies. *IEEE Access: Practical Innovations, Open Solutions, 7,* 184658–184667.

[16] Standard Test Method for Measuring the Electromagnetic Shielding Effectiveness of Planar Materials. *ASTM International Std. D4935-18*. https://standards.globalspec.com/std/4472766/astm-d4935-18

[17] Freudenberg Group. *EMI shielding for thermoplastic housing*. E-Mobility & Autonomous Driving. www.fst.com

[18] DSM Engineering Plastics. DSM provides a full spectrum of engineering plastics for electronic applications in the Connected Car, from www.dsm.com

[19] Agilent, E. N. A. (2008). 2, 3 and 4 Port RF Network Analyzers. Agilent Technol., Santa Clara, CA.

[20] Tserpes, K., Tzatzadakis, V., & Bachmann, J. (2020). Electrical conductivity

and electromagnetic shielding effectiveness of bio-composites. Journal of Composites Science, 4(1), 28.

[21] Więckowski, T. W., & Janukiewicz, J. M. (2006). Methods for evaluating the shielding effectiveness of textiles. Fibres & Textiles in Eastern Europe, (5 (59)), 18-22.

[22] Vasquez, H., Espinoza, L., Lozano, K., Foltz, H., & Yang, S. (2009). Simple device for electromagnetic interference shielding effectiveness measurement. IEEE EMC Soc. Newslett, 220, 62-68.

[23] Ren, F., Li, Z., Xu, L., Sun, Z., Ren, P., Yan, D., & Li, Z. (2018). Large-scale preparation of segregated PLA/carbon nanotube composite with high efficient electromagnetic interference shielding and favourable mechanical properties. Composites Part B: Engineering, 155, 405-413.

[24] Li, J., Zhang, G., Zhang, H., Fan, X., Zhou, L., Shang, Z., & Shi, X. (2018). Electrical conductivity and electromagnetic interference shielding of epoxy nanocomposite foams containing functionalized multi-wall carbon nanotubes. Applied Surface Science, 428, 7-16.

[25] Zeng, Z., Wang, C., Zhang, Y., Wang, P., Seyed Shahabadi, S. I., Pei, Y., Chen, M., & Lu, X. (2018). Ultralight and highly elastic graphene/lignin-derived carbon nanocomposite aerogels with ultrahigh electromagnetic interference shielding performance. ACS Applied Materials & Interfaces, 10(9), 8205–8213.

[26] Gao, W., Zhao, N., Yu, T., Xi, J., Mao, A., Yuan, M., ... & Gao, C. (2020). High-efficiency electromagnetic interference shielding realized in nacre-mimetic graphene/polymer composite with extremely low graphene loading. Carbon, 157, 570-577.

[27] Li, X., Yin, X., Liang, S., Li, M., Cheng, L., & Zhang, L. (2019). 2D carbide MXene Ti2CTX as a novel high-performance electromagnetic interference shielding material. Carbon, 146, 210-217.

[28] Barani, Z. (2020). Multifunctional Graphene Composites for Electromagnetic Shielding and Thermal Management at Elevated Temperatures. Advanced Electronic Materials., 6(11).

[29] Li, J., Ding, Y., Gao, Q., Zhang, H., He, X., Ma, Z., Wang, B., & Zhang, G. (2020). Ultrathin and flexible biomass-derived C@CoFe nanocomposite films for efficient electromagnetic interference shielding. Composites. Part B, Engineering, 190(107935), 107935.

[30] Kamchi, N. E., Belaabed, B., Wojkiewicz, J.-L., Lamouri, S., & Lasri, T. (2013). Hybrid polyaniline/nanomagnetic particles composites: High performance materials for EMI shielding. Journal of Applied Polymer Science, 127(6), 4426–4432.

[31] Hema, S. (2020). Effect of conducting fillers in natural rubber nanocomposites as effective EMI shielding materials. Materials Today: Proceedings, 25, 274–277.

[32] Thostenson, E. (2005). Nanocomposites in context. Composites Science and Technology, 65(3-4), 491–516.

[33] Daniel. (2006). Engineering mechanics of composite materials.

[34] Saini, P. (2015). Conjugated polymer-based blends, copolymers, and composites: Synthesis, properties, and applications. In Fundamentals of Conjugated Polymer Blends, Copolymers and Composites (pp. 1–118). John Wiley & Sons, Inc.

[35] Iijima, S. (1991). Helical microtubules of graphitic carbon. Nature, 354(6348), 56–58.

[36] Saini, P. (2013). Electrical properties and electromagnetic interference shielding response of electrically conducting thermosetting nanocomposites. In Thermoset Nanocomposites (pp. 211–237). Wiley-VCH Verlag GmbH & Co. KGaA.

[37] Saini, P., & Aror, M. (2012). Microwave absorption and EMI shielding behavior of nanocomposites based on intrinsically conducting polymers, graphene and carbon nanotubes. In A. D. S. Gomes (Ed.), New Polymers for Special Applications. InTech.

[38] Professor, E. S. (n.d.). Technology trends and electromagnetic compatibility

of integrated circuits. Archives-Ouvertes.Fr. Retrieved October 1, 2021, from https://hal.archives-ouvertes.fr/hal-02321017/file/EMCCompo2019-Sicard-v5-HAL.pdf

[39] Piersanti, S., de Paulis, F., Orlandi, A., Connor, S., Liu, Q., Archambeault, B., Dixon, P., Khorrami, M., & Drewniak, J. L. (2017). Near-field shielding performances of EMI noise suppression absorbers. IEEE Transactions on Electromagnetic Compatibility, 59(2), 654–661.

[40] Matsushita, N. (2003). Spin-sprayed Ni–Zn–Co ferrite films with high μr″>100 in extremely wide frequency range 100 MHz–1 GHz. Journal of Applied Physics., 93(10), 7133–7135.

[41] Saini, P., & Aror, M. (2012). Microwave absorption and EMI shielding behavior of nanocomposites based on intrinsically conducting polymers, graphene and carbon nanotubes. In A. D. S. Gomes (Ed.), New Polymers for Special Applications. InTech.

[42] ASTM D4935 - 18 Standard Test Method for Measuring the Electromagnetic Shielding Effectiveness of Planar Materials. (n.d.). Astm.Org. Retrieved September 29, 2021, from https://www.astm.org/Standards/D4935.htm

[43] Rohde-Schwarz.Com. Retrieved September 29, 2021, from https://scdn.rohdeschwarz.com

Ingeniería y Tecnología

3ciencias